

Instituto Tecnológico y de Estudios Superiores de Monterrey

Campus Monterrey

School of Engineering and Sciences



Evaluation of carbon fiber reinforced polymer composites
produced by Additive Manufacturing for design guidelines

A thesis presented by

Juan Miguel Naranjo Lozada

Submitted to the
School of Engineering and Sciences
in partial fulfillment of the requirements for the degree of

Master of Science

In

Manufacturing Systems

Monterrey Nuevo León, Mayo 11th, 2018

Dedication

This thesis is dedicated to my wife, Jenn, who is always my strength in any project of my life, and to my daughter, Amelia, who is my inspiration and motivation.

I also want to give a dedication to my parents, Alcivar and Marilub,
for its unconditional love and support.

To people who are part of research and development areas,
which with its work improves the people's life.

To God, for his infinite blessings

“People who live in the finite, live to overcome others, people who think about the
eternal, live to overcome themselves”

Daniel Habib

Acknowledgments

I want to thank greatly Dr. Horacio Ahuett-Garza, who is the advisor of the presented thesis work, as well as Prof. Pedro Antonio Orta Castañón, both for giving me the opportunity to be part of the Cyber-physical systems research group. Thanks for the academic guide that they have offered me, as well for providing the necessary resources for completing my initiatives.

I would like to express my deepest gratitude to all those who supported me in every aspect throughout my master's degree. Thank you very much to all of my colleagues and friends who were creators of new knowledge and great experiences.

Thanks to Tecnológico de Monterrey that has been provided support for my tuition; without its facilities would not have been possible to carry out the tests performed during this project.

Finally, I want to thank CONACYT for economic support throughout the entire process of my Master's degree, and the opportunity to belong in a research system and for motivating people to do a graduate program.

Evaluation of carbon fiber reinforced polymer composites using Additive Manufacturing for design guidelines

by

Juan Miguel Naranjo Lozada

Abstract

The use of additive manufacturing (AM) in many industries start to be a trend. The flexibility to manufacture complex geometries and the development of new AM materials and systems open new research fields. Recently, a family of technologies that produce fiber reinforced components has been introduced, widening the options available to designers. To find optimal structures using new AM technologies, guidelines for the design of 3D printed composite parts are needed. This thesis presents an evaluation of the effects that different geometric parameters have on the tensile properties of 3D printed composite. Two methods for manufacturing 3D printing composites, chopped and continuous fiber reinforcement (CFR), were analyzed. Parameters such as infill density and infill geometric patterns of chopped composite material, as well as fiber volume fraction and fiber arrangement of CFR composites are varied. The effect of the location of initial deposit point of reinforcement fibers on the tensile properties of the test specimens is also explored. From the findings, some design guidelines are proposed. Using these guidelines two application cases for Industry 4.0 systems were completed. A variation of the Rule of Mixtures (ROM) that provides a way to estimate the elastic modulus of a 3D printed composites is presented. Findings may be used by designers to define the best construction parameters for 3D printed composite parts.

Contents

Declaration of Authorship	Error! Bookmark not defined.
Dedication.....	i
Acknowledgments	ii
Abstract	iii
List of Figures	vi
List of Tables	viii
Chapter 1: Introduction	1
1.1 Motivation	2
1.2 Problem Statement and Context	4
1.3 Research Question.....	6
1.4 Solution overview	6
Chapter 2: State of The Art.....	8
2.1. AM Technologies and Manufactures	9
2.2. AM Materials	12
2.3. AM Fibers Reinforced Composites.....	16
2.4. Design for Additive Manufacturing	23
Chapter 3: Experimental Setup.....	27
3.1 Materials and Fabrication Process	28
3.2 Characterization Equipment	31
3.3 Experimental Setup 1: Nylon vs. Chopped Reinforced samples	33
3.4 Experimental Setup 2: Continuous carbon fiber reinforcement samples	34
3.5 Experimental Setup 3: Effect of initial point of reinforcement	35
Chapter 4: Results & Discussions	37
4.1 Experimental Setup 1: Nylon vs. Chopped Reinforced samples	38
4.1.1 Tensile Test Results of Experiment Setup 1	38
4.1.2 Sensitivity Analysis of Experiment Setup 1	39
4.1.3 Meso-structure Onyx Samples	42
4.1.4 Fracture Mechanism for Experiment Setup 1	43
4.2 Experimental Setup 2: Continuous Carbon fiber reinforced samples	44

4.2.1 Tensile Test Results Experimental Setup 2.....	44
4.2.2 Discussion Experimental Setup 2.....	46
4.2.3 Meso-structure CFR Samples	47
4.2.4 Fracture Mechanism Analysis for Experimental Setup 2	49
4.3 Experimental Setup 3: Effect of initial point of reinforcement	50
4.3.1 Tensile Test Results.....	50
4.3.2 Fracture Mechanism Analysis for Experimental Setup 3	51
4.3.3 Discussion Experimental Setup 3.....	53
4.4 3D Printed Composite Calculations	54
4.4.1 Composition of Onyx Samples	54
4.4.2 Volume Fraction for CFR Samples.....	57
4.5 Prediction of Elastic Modulus by Rule of Mixtures	59
Chapter 5: Design Guidelines and Recommendations	62
5.1 Design Guidelines for 3D printed composites.....	62
5.2 Recommendations.....	65
Chapter 6: Cases of Application	66
6.1 Case 1: Mechanical Design for Upgrade Equipment in Industry 4.0 system. ...	66
6.2 Case 2: Topology Optimization of FRC Bracket for a Vision System.	70
Chapter 7: Conclusions and Future Work.....	75
7.1 Conclusions.....	75
7.2 Future Work.....	76
Bibliography	78
Appendix A: Abbreviations and acronyms	81
Appendix B: Variables and Symbols.....	83
ANNEX 1: AM Manufactures and Equipment	84
ANNEX 2: Hybrid Technologies.....	90
Curriculum Vitae	91

List of Figures

Figure 1. Technology Road Map Additive Manufacturing for Automotive Industry	3
Figure 2. 3D printing fiber reinforced methods.....	16
Figure 3. Marktwo Printer at Tecnológico de Monterrey	18
Figure 4. Examples of AM lattice cells. Taken from [36].....	25
Figure 5. DFAM cases of study simulation and real AM parts from [37]	26
Figure 6. 3D Printed Specimens for a) Nylon b) Onyx and c) CFR.....	28
Figure 7. Fabrication of a) Onyx samples (Type 1 fiber embedding method) and	29
Figure 8. Application of cap strips on CFR samples	30
Figure 9. Tensile Test a) Onyx sample b) CFR composites	31
Figure 10. SEM microscopy samples a) Fracture specimens b) 1R vs. 3R.....	32
Figure 11. Onyx sample during an FTIR analysis.....	33
Figure 12. Strain-stress curves for 3d printed Nylon, Onyx and CFR composites.	38
Figure 13. Effect in Elastic Modulus due to material.....	39
Figure 14. Effect in Tensile Strength due to material.....	39
Figure 15. ANOVA results for Elastic Modulus	40
Figure 16. ANOVA results for Tensile Strength	40
Figure 17. ANOVA factorial plots for Experimental Setup 1	41
Figure 18. Infill Geometries and Density tested in ONYX samples.....	43
Figure 19. Close-up of failure mechanism of a) Nylon specimen; b) Onyx sample.....	44
Figure 20. Effect in Elastic Module with respect to Fiber Volume Fraction	45
Figure 21. Effect in Tensile Strength with respect to Fiber Volume Fraction	45
Figure 22. Effect in Elastic Module with respect to sample configuration	46
Figure 23. Effect in Tensile Strength with respect to sample configuration	47
Figure 24. a) 1R layer top view b) 3R layer top view from SEM microscopy	47
Figure 25. Measures from Stereo ZEIS optical microscopy.....	48
Figure 26. Measurements from SEM microscope at a) 1R layer b) 3R layer.....	49
Figure 27. Close-up of failure mechanism of CFR sample	49
Figure 28. Break zones in the specimens 1R-12L.....	50
Figure 29. Specimens and schematics of 1R-12L with different start points at	51
Figure 30. Outside Fracture mechanism.	52

Figure 31. Inside Fracture mechanism	53
Figure 32. FTIR spectrums for Nylon and Onyx samples	55
Figure 33. FTIR spectrum for Polyamide (Nylon 6). [48].	55
Figure 34. CFR specimen a) Top view b) Cross Section A-A.'	58
Figure 35. Cost vs. Strength Experimental Setup 1	63
Figure 36. Cost vs. Strength Experimental Setup 2.....	63
Figure 37. Mechanical design Smart audio system a) Support structure b) Assembly ..	67
Figure 38 AM composites features incorporated during design.....	68
Figure 39 3D printed support structure for Smart audio system	70
Figure 40. Hypermesh interface with TO and FEA setup for Analysis 2.	72
Figure 41. Overall TO and FEA results for different Design Space Geometry	73
Figure 42. Optimized Bracket for Vision System. a) CAD b) Slicing software Setup	73
Figure 43. Smart Vision System a) Final Assembly b) Printed bracket.....	74

List of Tables

Table 1 Classification of AM Technologies adapted Hybrid Mfg. Technologies [15].....	9
Table 2. Commercially AM materials used in AM processing. Adapted from [16].....	12
Table 3. Commercially alloys used in AM processing. Adapted from [21]	14
Table 4. Literature review FCR manufacturing by AM	19
Table 5. Morphological Matrix FCR manufacturing by AM	21
Table 6. Specimen Dimensions for Type I geometry ASTM D638-14	30
Table 7. Printer Parameters defined in Slicing Software	34
Table 8. Printer Parameters defined in Slicing Software	34
Table 9. Printer Parameters defined in Slicing Software	35
Table 10. Experimental Setups and main Printer Parameters	36
Table 11. Results from Tensile Test (ASTM D638) Nylon vs. Onyx Samples	38
Table 12. Results from Tensile Test (ASTM D638) for CFR samples	44
Table 13. Results from Tensile Test (ASTM D638) for Experimental Setup 3	51
Table 14. Results from FTIR spectrum analysis of Onyx.....	57
Table 15. Volume Fraction calculations for Experimental Setup 2.....	58
Table 16. Results from Prediction Model by Rule of Mixtures	60
Table 17. Fit analysis results for magnets (shaft) inside the base part	69

Chapter 1: Introduction

Since rapid prototyping was introduced in the eighties, many additive manufacturing processes have been developed. In the early stages, rapid prototyping was used to create physical models to verify manufacturability functions and to perform design and form-fitting checks. However, it was not until recent years that additive manufacturing technologies started to produce functional parts. Some of the new technologies developed are selective laser sintering (SLS), direct metal laser sintering (DMLS), selective laser melting (SLM), laser engineered net shaping (LENS), fused deposition modeling (FDM), electron beam melting (EBM).

The availability of more materials and different processing technologies resulted in what is currently known as Additive Manufacturing (AM) or 3D printing. Suppliers of these technologies have appeared in response to a market that shows a high acceptance of the machines and services. According to Wohlers Associates, the expected revenue for the AM market in 2020 will be 10.8 billion USD. This is a conservative projection given that in

2016 Wohlers Report showed that the Additive Manufacturing Industry surpassed \$5.1 billion in 2015 when the expected revenue was only 4 billion. [1].

Component suppliers pursue AM applications in the automotive and aerospace industries. Although different industrial sectors have shown a great deal of interest in additive manufacturing systems, product quality and reliability of 3D printed parts are still a concern. However rigorous performance requirements have posed problems for the introduction of AM parts in the final products. Additionally, the replacement of traditional processes by AM is still not attractive for most industries. For the current traditional geometries and materials, AM does not provide substantial advantages. Currently, AM trends conclude that Design for Additive Manufacture is a requirement for the implementation of this type of AM technology [2].

A particular field of application that offers potential advantages of AM technologies is fiber reinforcement composites (FRC). These materials have begun to be studied for civil and mechanical structures and can be used for engineering purposes [3]. To obtain functional FRC structures, the designer must consider several processes and design parameter.

1.1 Motivation

A trends analysis was conducted by an undergraduate group of the Strategic Prospective class during the August-December 2016 semester at Tec de Monterrey, Campus Monterrey [4]. The analysis concluded that:

- The worldwide technology trends now are oriented to connectivity (big data and data cloud) and bio and nanotechnologies.
- In 2022, the concepts of Industry 4.0 and Internet of the Things are projected to be essential in all the industries.
- In 2025 the concepts of customization and digitalization of the products will be used in the production systems.

- To introduce all these concepts, one of the enabling technologies is the Additive Manufacturing. AM provides flexibility in the products and fabrication processes.

AM is closer to becoming a reality for manufacturing functional parts and increasing its presence in the automotive sector. A technology roadmap for the AM in the automotive industry was prepared for this study. The result is described in Figure 1. Soon, the use of AM metal and plastic parts will be common. This technology will become essential in the automotive industry for ease of manufacture, low costs, use of multiple materials and speed of production. In spite of all the advantages of AM, after a complete analysis, there are issues that need to be addressed.

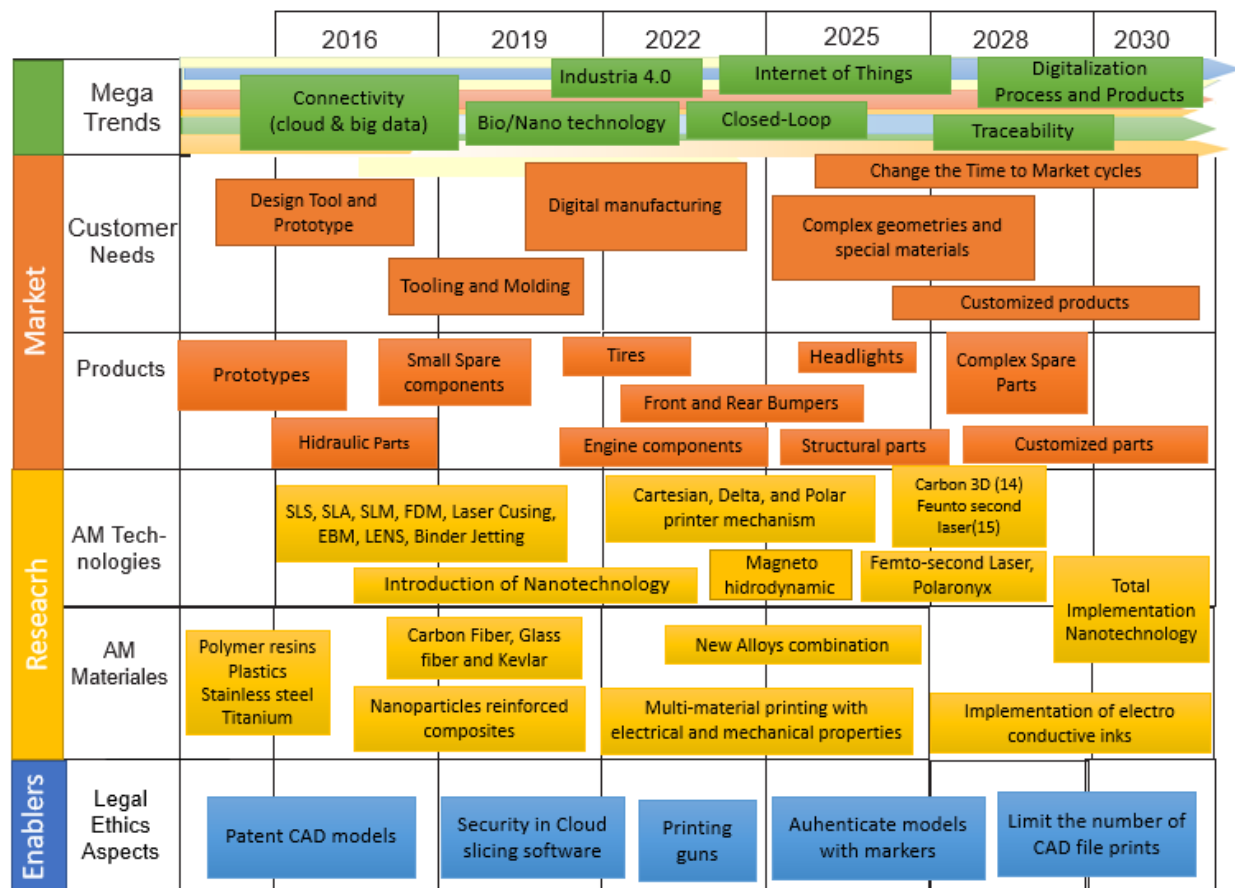


Figure 1. Technology Road Map Additive Manufacturing for Automotive Industry

Two trends were detected in the AM technology field. One oriented to enable the use of the current machines with more materials focusing on obtaining better performance of final parts. The second trend is oriented to finding new technologies that overcome the limitations of current systems. The AM materials are the most studied field right now. The main materials studied are titanium and steel alloy for AM in metals. For plastics, the use of carbon fibers and nanoparticles with polymers matrix starts to be a trend [2].

According to Mallick [5] fiber-reinforced polymer composites, like carbon fiber with nylon, have a huge number of commercial and industrial applications. They can be used in electronics (e.g., printed circuit boards), building construction (e.g., floor beams), furniture (e.g., chair springs), power industry (e.g., transformer housing), oil industry (e.g., offshore oil platforms and oil sucker rods used in lifting underground oil), medical industry (e.g., bone plates for fracture fixation, implants, and prosthetics), and in many engineering fields.

The imminent introduction of Industry 4.0 and Internet of the Things inside the factories, the large number of commercial and industrial uses of fiber-reinforced polymer composites, and the customization and digitalization of the products create the perfect scenario to trigger the use of 3D printed composites in the industry. However, the mechanical properties of composites materials are strongly affected by the fabrication process. A better understanding of the relationship between process and final properties is necessary.

1.2 Problem Statement and Context

Current trends show that AM was left to use only in prototyping, some applications in jigs, fixtures, tooling, and molding are reported [6][7][8][9]. It is expected that in the middle term aerospace and automotive industries will start to use AM for low production functional parts [10][11].

The accuracies obtained in AM are far from traditional process. Post-processing operations are needed to obtain tight tolerances. Limited part size, printing envelopes,

and speed of the process are also obstacles for metal AM machines. Also, very expensive material costs compared with the traditional process were presented. Recently, new technologies that can print fiber reinforced components have been introduced, widening the options available to designers.

Currently, AM researchers are focusing in develop optimal process parameters (speed, laser power, particle size, etc.) for metals [12][13][14]. For plastics, the technology is more developed, and the process parameters such as temperature or speed are well known and defined by the equipment's manufactures. But the AM parts still exhibit different mechanical properties compared to the same parts in traditional processes, showing that a research gap in the process still exists.

Most of the commercial plastic AM equipment have restrictions to change process parameters as speed or temperature. In contrast, most of the slicing software used to convert the CAD designs into printing layers, offer several geometric parameters options as infill density, infill pattern, layers thickness, etc. For AM fiber reinforcement composites, some geometric patterns such as the alignment of the fiber or the printing architecture change the final properties of the parts. Some design guidelines for the optimization of 3D printed composite parts are needed.

In general, the current problem with 3D printing composites parts is that some design rules are needed to fully exploit the benefits of AM. To define these rules, process parameters, like speed or temperature cannot be modified in commercial equipment. On the other hand, several geometric parameters can be modified into slicing software to improve the final mechanical properties.

1.3 Research Question

AM fiber reinforced composite processes can produce engineering parts. The effect that fabrication and geometric parameters have on the final mechanical properties need to be studied.

Design for Additive Manufacture can introduce new features that produce viable AM applications.

1.4 Solution overview

In the case of fiber reinforced 3D prints, a completely new field of study is open due to the orthotropic behavior of the material. For the fabrication of 3D printed composites, several geometric parameters influenced the final mechanical properties.

The present thesis work proposes a complete evaluation of the tensile properties of 3D printed composites to overcome the research gap in FRC. Three experimental setups that characterize the mechanical behavior of 3D printed composites were conducted. Two different AM processes for fabrication of fiber reinforced composites, continuous carbon fiber and chopped carbon fiber reinforcements, were studied. From the experimentation, the findings were used to propose some design guidelines that help the engineer to define the best parameters for the print part. Finally, some application cases using these findings were completed. The optimized AM components showed substantial advantages by introducing carbon fiber reinforcement.

The proposed approach uses the know-how of the AM manufactures in process parameters and focuses on the design parameters. The findings in the experimental setups and the design guidelines proposed in this thesis contribute to close the gap between the AM technology and its potential applications in the industry.

This thesis work is organized into six chapters as follows:

Chapter 1 provides the introduction, the motivation, the research question and the solution overview to the problem studied.

Chapter 2 covers a State of Art review of current AM technologies focuses on 3D printed fiber reinforced composites.

Chapter 3 collects the methodology used for the different experimental setups.

Chapter 4 summarizes the results and discussions of the experimental setups conducted during this thesis work.

Chapter 5 collects the design guidelines and the recommendations found during this study.

Chapter 6 present two cases of application: a support structure in the upgrade of an equipment in Industry 4.0 and a topology optimization bracket in a smart vision system.

Finally, Chapter 7 shows the Conclusions and proposed Future Work.

Chapter 2: State of The Art

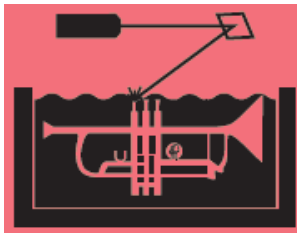
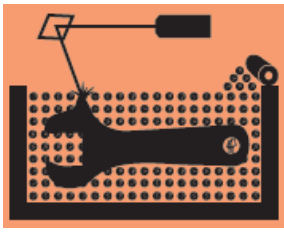

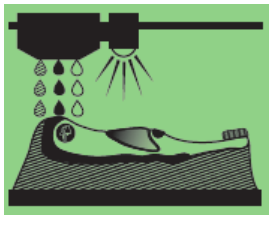
This chapter summarizes the main technology families for Additive Manufacturing (AM) and shows the principal materials available for AM. The literature review focus on 3D printed fiber reinforced composites (FRC). A detailed morphological analysis is presented for the different methods of FRC fabrication and its applications.

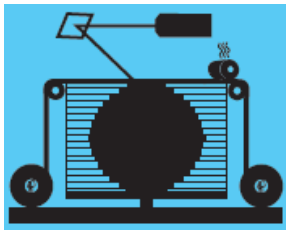
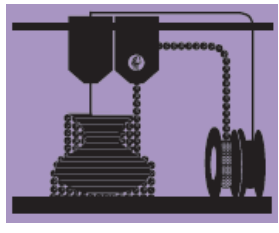


Additional, a literature review about Design for Additive Manufacturing (DFAM) was conducted, and the principal trends and some applications related to FRC components are presented in this section.

2.1. AM Technologies and Manufactures

As mentioned before, in recent years many AM technologies have been developed, and new systems are introduced each year. For a better understanding of the different AM systems, this study presents in Table 1 the classification of AM technologies according to the norm ASTM F2792 which groups the various technologies in seven families. Hybrid technology is classified in a different category.

Table 1 Classification of AM Technologies adapted Hybrid Mfg. Technologies [15]

7 Families of Additive Manufacturing (ASTM F2792)			
			
VAT PHOTOPOLYMERIZATION	POWER BED FUSION (PBF)	BINDER JETTING	MATERIAL JETTING
Alternative Names: SLA, DLP, CLIP	Alternative Names: SLS, DMLS, SLM, EBM	Alternative Names: 3DP, ExOne, Voxeljet	Alternative Names: Polyjet, SCP, MJM, Projet
A vat of liquid photopolymer resin is cured by selective exposure to light which initiates polymerization and converts the exposed areas to a solid part	Powdered materials are selectively consolidated by melting it together using a heat source as a laser or electron beam. The unfused material surrounding the solid part acts as support material.	Liquid bonding agents are selectively applied onto thin layers of powdered material to build up parts layer by layer. Metal or ceramic "green" parts are typically in a furnace after they are printed.	Droplets of material are deposited layer by layer to make parts. Common varieties include jetting a photocurable resin and curing with a UV light, and thermally molten materials that solidify in ambient temperatures.
Strengths: High level of accuracy and complexity Smooth surface finish Accommodates large build areas	Strengths: High level of complexity Powder acts as support material Wide range of materials	Strengths: Allows for full-color printing High productivity Uses a wide range of materials	Strengths: High level of accuracy Allows for full-color printing Enables multiple materials
Materials: UV curable photopolymer resins	Materials: Plastics, Metal and Ceramic Powders, and Sand	Materials: Plastics, Metal and Ceramic Powders, and Sand	Materials: Photopolymers, polymers, waxes.

			
SHEET LAMINATION	MATERIAL EXTRUSION	DIRECTED ENERGY DEPOSITION (DED)	HYBRID
Alternative Names: LOM, SDL, UAM	Alternative Names: FFF, FDM	Alternative Names: LMD, LENS, DMD	Alternative Names: AMBIT
Sheets of material are stacked and laminated together to form an object. The lamination method can be adhesives or chemical, ultrasonic welding, or brazing. Unneeded regions are cut out layer by layer and removed after the object is built.	The material is extruded through a nozzle or orifice in tracks or beads, which are then combined into a multi-layer model. Common varieties include heated thermoplastic extrusion and syringe dispensing.	Powder or wire is fed into a melt pool which has been generated on the surface of the part where it adheres to the underlying part or layers by using an energy source such as a laser or electron beam. This is essentially a form of automated build-up welding.	Laser metal deposition (a form of DED) is combined with CNC machining, which allows additive manufacturing and subtractive machining to be performed in a single machine so that parts can utilize the strengths of both processes.
Strengths: <ul style="list-style-type: none"> • High volumetric built rates • Relatively low cost • Allows for combinations of metal foils including embedding components 	Strengths: <ul style="list-style-type: none"> • Inexpensive and economical • Allows for multiple colors • Office environment • Parts have good structural properties 	Strengths: <ul style="list-style-type: none"> • Not limited by direction or axis • Effective for repairs and adding features • Multiple materials in a single part • Highest single-point deposition rates 	Strengths: <ul style="list-style-type: none"> • Smooth surface finish • High productivity • Geometrical and material freedoms • Automated in-process support removal, finishing, and inspection
Materials: Paper, Plastics Sheets, and Metal Foils/ Tapes	Materials: Thermoplastics filaments and pellets, liquids and slurries (syringe types)	Materials: Metal wire and powder, with ceramics.	Materials: Metal wire and powder, with ceramics.

Currently, there are dozens of technologies and companies working in additive manufacturing with numerous applications and materials. Detailed information on the machines, characteristics, capacities, potential applications are described in Annex 1 AM Manufactures and Equipment.

For metal AM components, Powder Bed Fusion systems is the most developed technology, followed by Direct Energy Deposition machines. In a small number, Binder Jetting systems also could found. In Powder Bed Fusion machine, SLM (Selective Laser Melting) is the most extended technology, a trend that was also found in the literature review. However, there are new developers like Markforged, Desktop Metal, and Exone that enable the use of other technologies (non-laser based technologies) [2].

In the case of polymers, Material Extrusion machines look like the most extended technology. However, its low speed is a limitation to introduce this type of equipment in mass production. On the other hand Material Jetting and Vat Polymerization seem to have reappeared with companies like Stratasys (Polyjet) and Carbon 3D (SLA) respectively. These last technologies have a higher printing speed but also need postprocessing work [2].

As can see in Annex I, it was found that machine manufacturers are focusing on the development of mass production equipment, although all are limited to small parts. A limited number of machines are oriented to research or special applications, such as jewelry or dental replacement.

Finally, it is important to notice that almost all the main manufacturers and developers of AM technologies are located in the United States and Germany, and just a few (Stratasys, 3D Systems, and Markforged) have local representatives in Mexico.

2.2. AM Materials

Currently, a variety of AM materials are available for different applications, some of the most relevant materials are described in Table 2.

Table 2. Commercially AM materials used in AM processing. Adapted from [16]

Material type	AM technology	Manufacturer	Materials
Photopolymer resin	SLA	3D Systems	Variety of epoxy resins and nano-composite resin
	Envisiontec Perfactory	Envisiontec	Epoxy-acrylic resins, nano-composite resin and acrylic resin (investment casting)
	PolyJet (3D printing)	Stratasys (Object)	Proprietary photopolymers and biocompatible resins
Plastic	SLS	3D Systems	VisiJet® SL Black VisiJet® SL Clear VisiJet® SL Flex VisiJet® SL Impact VisiJet® SL Jewel VisiJet® SL Tough
	SLS	EOS GmbH	Alumide, PA 1101, PA 1102 black, PA 2200, PA 2201, PA 3200 GF, PrimeCast 101, PrimePart FR (PA 2241 FR), PrimePart PLUS (PA 2221
	FDM	Stratasys	ASA ABSM30™ ABSM30i™ ABSES7™ PC-ABS PC-ISO™ PC ULTEM-9085 resin ULTEM-1010resin PPSF FDM Nylon12™ FDM Nylon 6™ ST-130™
	FFF	Markforged	Carbon Fiber, Kevlar®, Fiberglass, Nylon, Onyx, and High-Strength, High-Temperature Fiberglass
	Digital Light Synthesis	Carbon 3D	RPU: Rigid Polyurethane FPU: Flexible Polyurethane EPU: Elastomeric Polyurethane EPX: Epoxy
Metal	DMLS	EOS GmbH	Stainless steel GP1 and PH1, cobalt chrome SP1 and SP2, titanium Ti64, Ti64 ELI and Ti CP, maraging steel MS1, AlSi20Mg and EOS Inco718
	SLM	MTT	Stainless steel and titanium
	Laser Cusing	Concept Laser	Stainless steel, hot-work steel, titanium TiAl6V4, aluminum AlSi12, AlSi10Mg and nickel-based alloy (Inconel 718)
	EBM	Arcam AB	Pure titanium, Ti6Al4V, Ti6Al4V ELI and cobalt chrome

Some of the principal applications of materials in Table 2 are:

- Stainless steel GP1 and PH1: For medical devices, implants and functional parts.
- Cobalt chrome MP1: Biomedical implants and fine functional parts.
- Cobalt chrome SP2: Dental restorations and medical applications (SP1).
- Titanium Ti64, Ti64 ELI, and Ti CP: Functional parts and biomedical implants.
- Maraging steel MS1: Heavy duty molds

To examine the suitability of AM components that may compare well with the conventional material in traditional subtractive manufacturing processes several factors must be considered. AM materials have different mechanical properties and final accuracies depending on raw material characteristics (ex. grain powder sizes, purity). AM technology (ex. SLM, SLS, LENS, LASER CUTTING), and the process parameters (ex. laser power, speed, printing architecture) also have an important effect on final performance [2]. It is mandatory for a design engineer to know the material options and corresponding process parameters

2.2.1. Metal AM materials

Currently, metal AM materials do not offer advantages when compared to traditional processes. From five AM cases of study conducted by a graduate group of the Technology Innovation Foresight class during the January-May 2017 semester at Tec de Monterrey, Campus EGTP [17][18]. High costs of equipment were found. Very long times compared to traditional process (ex. Die casting, powder metallurgy, etc.) were presented. Expensive material costs were also reported with a graduate class. Now is not feasible to manufacture big or large functional parts. For small functional products, the technology is available, but feasibility depends on parts demand and response time.

To exploit the advantages of AM, a field that has special attention is the printing of alloys, intermetallic, and bimetal for specific applications. For example [19] Fraunhofer-

RWTH Aachen University reported some basics experimental setups to manufacture tools with combined materials. The idea is to manufacture the core of the tool insert from hot work steels (1.2343 or 1.2709) using SLM. During this process, cooling channels with complex geometries are integrated into the exact places where they are needed to heat or cool the component. Then an external shell with a harder material (tungsten) can be added as a coating by laser cladding. Currently, this process is in research state and does not produce functional parts.

Murr et al. [20] report that considerable efforts have been made worldwide in the development, technology, and applications of intermetallic Ti Al-based alloys at high-temperatures for long-term operation. Applications include propulsion exhaust system components and aero-engine compressor blades. Other aerospace and automotive applications have also been examined in recent years. The replacing of heavier nickel-based superalloys for the next generation of aircraft engines, space vehicles, and automotive engine components are studied. Also, some research is conducted in turbine wheels and engine exhaust valves and pistons for improved auto fuel economy.

Some commercial alloys already available are reported in Table 3. In the case of alloys processing, the Powder Bed Fusion systems are considered the best option. The alloys can be easily implemented by controlled amounts of each powder element in the printing process.

Table 3. Commercially alloys used in AM processing. Adapted from [21]

Titanium	Aluminum	Tool Steels	Super Alloys	Stainless steel	Refractory
Ti-6Al-4V	Al-Si-Mg	H13	IN625	316 & 316L	MoRe
ELI Ti	6061	Cermets	IN718	420	Ta-W
CP Ti			Stellite	347	CoCr
γ Ti Al				PH 17-4	Alumina

In general for metal AM materials, state of the art shows that the technology is in a first research stage. The research focus is the development of optimal process parameters (speed, laser power, particle size, etc.).

2.2.2. Polymer AM materials

In contrast to metal AM materials, during the past decades, AM polymer manufacturers have been made great progress in developing new and better materials. Currently, the technology is more mature and the process parameters (speed, temperatures, times, etc.) are well known for the manufactures.

Most AM suppliers have an extensive portfolio of polymers materials like ABS or PP, but the mechanical properties can be differing from expected mechanical properties obtained by injection or extrusion process. To reach mechanical properties required for the specific application the development of new polymers materials starts to be a trend. For example, Acrylic stereo-lithography materials, which exhibit limited engineering properties, have been replaced by improved epoxy-based photo-polymers[21].

In the same way, several efforts have been made to overcome the limitations of FDM parts with the addition of fiber or particle reinforcement. Stratasys recently launched its FDM Nylon 12CF, a carbon fiber-filled thermoplastic, which contains 35% chopped carbon fiber by weight. Stratasys [22] report that has the highest flexural strength of any FDM thermoplastic, resulting in the highest stiffness-to-weight ratio. This new type of materials create a completely new field of study: AM fibers reinforced composites.

2.3. AM Fibers Reinforced Composites

2.3.1. Fabrication types of AM FRC

According to Prüß, H. et al. [23] three methods of fiber implementation based on the embedding of the fiber could be defined. Figure 2 shows the schematics of each type of AM fabrication process.

- 1) Embedding before the printing process, that is, the filament itself is a composite,
- 2) Embedding in the print head, meaning, two materials are combined when they pass through the extruder.
- 3) Embedding on the component, thus requiring two or more independent extruders, each one with an independent nozzle.

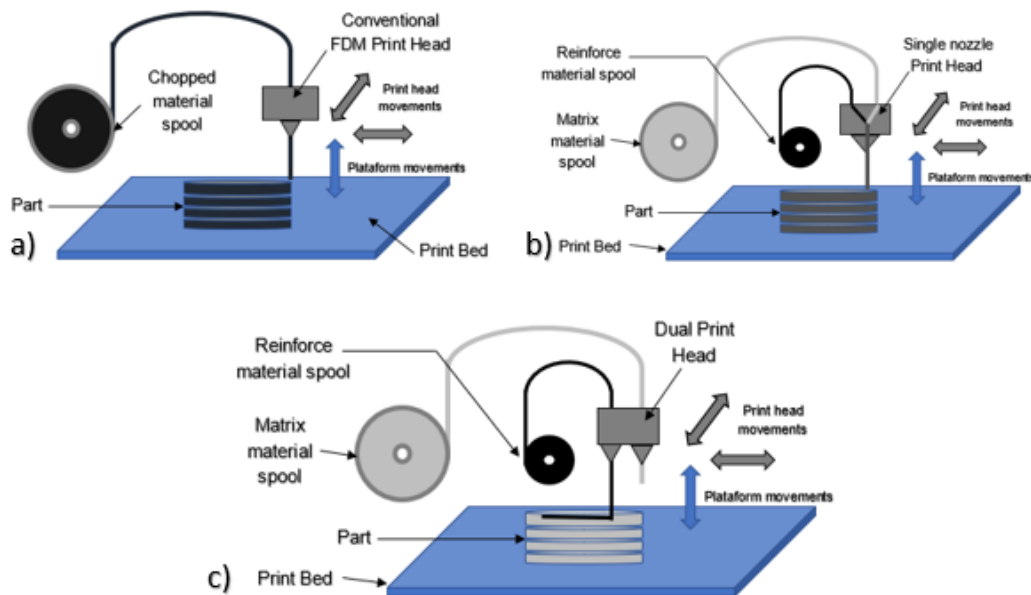


Figure 2. 3D printing fiber reinforced methods a) Embedding Before the Printing Process b) Embedding in the Print Head. c) Embedding on the component.

This classification is relevant because the properties of the part depend not only on the volume fraction of the reinforcing fiber but also on the manner in which the fibers are

deposited. Baumann et al. [24] reported that from the three types, third method (embedding on the component) results in a considerable increase in tensile strength and elastic modulus for different cases of continuous carbon fibers reinforced polymers. There is a growing interest in these processes due to their potential to produce functional parts for engineering applications.

2.3.2. Marktwo Fabrication Process

Recently, Markforged [25] introduced the Marktwo printer (Figure 3) which can manufacture continuous fiber-reinforced polymers (Type 3, embedding on the component). The equipment also prints chopped composites with its new filament, Onyx that contains chopped carbon fibers (Type 1, embedding before the printing process).

For chopped carbon reinforced composites, the Onyx filament is loaded as matrix material; the printing process is similar to a conventional FDM printer. The dual printing head uses only the plastic nozzle (Figure 2a.), the filament is fed through the nozzle that melts, extrudes and deposits it, layer by layer, in the desired shape, while the moving platform is lowered after each layer is deposited.

The printing process for continuous reinforced composites consists of two stages, each of which is performed by a separate nozzle in the dual printer head (Figure 2c.). The nylon filament is printed first, and the reinforcing fiber is deposited in a second stage within the same layer. According to Mark [26] nylon is printed with a hot end temperature of 263 °C onto a non-heated print bed while the fiber reinforced composite filament is heated in a transverse pressure zone to a temperature higher than the melting temperature of the matrix material to melt the matrix material interstitially within the filament. The head applies an ironing force to the melted matrix material.

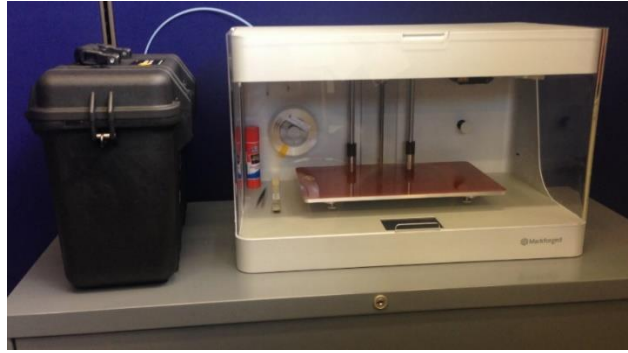


Figure 3. Marktwo Printer at Tecnológico de Monterrey

The specifications and materials available for Marktwo printer are the following:

- Work area: 320mm x 132mm x 154mm
- Resolution: 100 Microns
- Matrix Materials: Nylon and Onyx
- Reinforced Materials: Carbon Fiber, Kevlar®, Fiberglass, Nylon, Onyx and High-Strength, High-Temperature Fiberglass.

2.3.3. State of the Art & Morphological Analysis of FRC Research

Table 4 summarizes state of the art in FRC that uses AM technologies. The table includes the authors, universities, and journals that published articles in this field. The AM materials, AM technologies, and Focus topic are included for each article analyzed.

From the articles studied in Table 4, the first five papers were compared with the present thesis approach. The similar characteristics and novelty aspects are presented in a morphological matrix (Table 5).

Table 4. Literature review FCR manufacturing by AM

	Authors	Year	Title	University	Journal	Materials	AM tech.	Focus on
1	Andrew N. Dickson *, James N. Barry, Kevin A. McDonnell, Denis P. Dowling	2017	Fabrication of continuous carbon, glass and Kevlar fibre reinforced polymer composites using additive manufacturing	University College Dublin, Ireland	Additive Manufacturing	Nylon + CF+ Kevlar+ GF	FDM	Mechanical Properties in base of VF for CFR
2	Garrett W. Melenka a, Benjamin K.O. Cheung a, Jonathon S. Schofield a, Michael R. Dawson b, Jason P. Carey	2016	Evaluation and prediction of the tensile properties of continuous fiber-reinforced 3D printed structures	University of Alberta, Canada	Composite Structures	Nylon + Kevlar	FDM	Prediction of Youngs Modulus in base of VF for CFR
3	Fuda Ning, Weilong Cong, Yingbin Hu and Hui Wang	2017	Additive manufacturing of carbon fiber-reinforced plastic composites using fused deposition modeling: Effects of process parameters on tensile properties	Tech University, Lubbock, TX, USA	JOURNAL OF COMPOSITE MATERIALS	Chopped CF +ABS	FDM	Tensile Properties in base of process parameters
4	Frank van der Klift ¹ , Yoichiro Koga, Akira Todoroki, Masahito Ueda, Yoshiyasu Hirano, Ryosuke Matsuzaki	2016	3D Printing of Continuous Carbon Fibre Reinforced Thermo-Plastic (CFRTP) Tensile Test Specimens	Delft University of Tech, The Netherlands Tokyo University of Science, Japan	Open Journal of Composite Materials,	Nylon + CF	FDM	Tensile Properties in base of VF for CFR
5	J. Justo, L. Távara*, L. García-Guzmán, F. París	2017	Characterization of 3D printed long fibre reinforced composites	Universidad de Sevilla	Composite Structures	Nylon + CF/ Fiberglass	FDM	Tensile & Compression Test

6	Xin Wang a, Man Jiang b, Zuowan Zhou b, Jihua Gou a, *, David Hui c	2016	3D printing of polymer matrix composites: A review and perspective	University of Central Florida, USA	Composites Part B	Nylon/ ABS Epoxy, carbon nanofibers	FDM, SLA, DLP, SLS	Prospective Study
7	Christoph Klahn*, Bastian Leutenecker, Mirko Meboldt	2014	Design for Additive Manufacturing – Supporting the Substitution of Components in Series Products	ETH Zurich, Switzerland	24th CIRP Design Conference	Several	SLM SLS	DFMA
8	Hauke Pruß, Thomas Vietor	2015	Design for Fiber-Reinforced Additive Manufacturing	Technische Universität Braunschweig, Germany	JOURNAL OF MECHANICAL DESIGN.	Nylon/ ABS Epoxy, carbon nanofibers	FDM, SLA, DLP, SLS	DFMA
9	Susanne C, Martin Schnabel, Elke Vorndran, Jürgen Groll, Uwe Gbureck	2014	Fiber reinforcement during 3D printing	University Hospital Würzburg, Germany	Materials Letters	Gypsum +PAN +PA +GF	Binder Jetting ZPrinter 310	Medical Application 3D printed composites
10	Xiaoyong Tian , Tengfei Liu, Chuncheng Yang, Qingrui Wang, Dichen Li	2016	Interface and performance of 3D printed continuous carbon fiber reinforced PLA composites	Xi'an Jiaotong University, China	Composites: Part A	PLA + CF	FDM (open source printer)	Tensile Properties in base of process parameters
11	M.Sc. Florian Baumann*, M.Sc. Julian Scholz, Prof. Dr.-Ing. Jürgen Fleischer	2017	Investigation of a new approach for additively manufactured continuous fiber-reinforced polymers	Institute of Production Science, Karlsruhe, Germany	1st Cirp Conference Composite Materials Parts	Nylon + CF + GF	FDM	Tensile Properties in base of VF for CFR
12	Clayson C. Spackman, Christopher R. Frank, Kyle C. Picha, Johnson Samuel*	2016	3D printing of fiber-reinforced soft composites: Process study and material characterization	Rensselaer Polytechnic Institute, 110 8th Street, Troy, NY 12180, USA	Journal of Manufacturing Processes	Nylon + CF	Electro-spinning in UV curing resin	Tensile Properties in base of process parameters

Table 5. Morphological Matrix FCR manufacturing by AM

Factor	Characteristics	Thesis	1	2	3	4	5
Materials	<u>Chopped Composites</u>	x			x		
	Nylon as Matrix	x	x	x		x	x
	Fiber Carbon Reinforcement	x	x		x	x	x
	Fiber Glass Reinforcement		x				x
	Kevlar Reinforcement		x	x			
Type of Printer	Markone/Marktwo	x	x	x		x	x
	Other FDM printer				x		
Measurements reported	Youngs Modulus	x	x	x	x	x	x
	Tensile Strength	x	x		x		x
	Flexural Modulus		x				
	Others: Toughness Ductility				x		x
Parameters evaluated	Process Parameters (speed, T)				x		
	<u>Infill density and geometry</u>	x					
	Reinforcement Volume fraction	x	x			x	
	Orientation of the fibers		x		x		x
	<u>Arrangement of the reinforced fiber</u>	x					
	<u>Start point effect in Fracture</u>	x					
Prediction models	Rule of Mixtures	x	x			x	
	Orthotropic Matrix Model			x			
Microscopy	SEM/ Optical/ Stereo ZEISS	SEM/ SZ	0	0	SEM	0	0

From Table 5, the novelty of our approach is to evaluate the effects that geometrics parameters have on the final mechanical properties of AM reinforcement composites. Additional a numerical comparison of the mechanical properties between chopped composites and continuous fiber reinforced composites are reported.

2.3.4. Results for Research Investigations in FCR

The fabrication of continuous carbon, glass and Kevlar fiber reinforced polymer composites on a Markone printer model was reported by Dickson et al. [27]. They evaluated the tensile and flexural properties of test specimens with carbon fiber reinforcement and concluded that these materials could reach tensile strengths of up to 368 MPa, which exceeds the strength of some conventional structural materials, such as Aluminum 6061-T6. They also analyzed the effect of the increase of volume fraction of glass fiber on tensile properties of the material.

In this field, some authors report efforts to predict the mechanical properties of this type of composites. For example, Melenka et al. [28] presented an evaluation of the tensile properties of Kevlar 3D printed structures and tried to predict the elastic modulus using an orthotropic stiffness matrix. Van der Klift et al. [29] presented an evaluation of tensile properties for two carbon fiber 3D printed specimens and tried to predict the elastic modulus by the rule of mixtures of composites. The two mathematical models only are precise in a specific range of fiber volume fraction content. In the present thesis work, several cases with a larger fiber volume fraction content range were tested. The approach for the prediction of elastic modulus presented in this study merges the two previous methods and analyzes the why of the inaccuracies in different ranges of volume fraction content.

Additional investigations for fiber reinforcement during 3D printing were conducted for medical applications like those reported by Christ et al. [30]. Other articles analyze the effect of process parameters on final mechanical properties, such as the case of Yang et al.[31] and Spackman et al.[32]. Others matrix materials are also studied. Ning et al. [33] evaluated the mechanical properties of ABS polymers combined with chopped carbon fibers, as a function of FDM printing process parameters. Their goal was to improve the tensile strength of the parts based on obtained the best process parameters. Most of the researchers still focus on process parameters or new material developments. However commercial plastic AM equipment has restrictions to change process parameters as speed or temperature. On the other hand, the industries that own AM equipment are

allowed through software to change several geometric parameters options as infill density, infill pattern, layers thickness, etc. The effect that these geometric parameters have on the final properties of the parts is a research gap, especially for AM fiber reinforcement composites.

In spite of all progress, Arcos-Novillo and Güemes [34] have argued that replacing traditional processes with AM is still not attractive for many mass production applications, mainly because of the expensive initial investment, higher material costs and production times compared to traditional process. To overcome these limitations, a new research field starts to be a trend: Design for Additive Manufacturing (DFMA).

2.4. Design for Additive Manufacturing

According to Thompson M. et al. [11], DFAM is the practice of designing and optimizing a product together with its production system to reduce development time and cost and increase performance, quality, and profitability. Thompson et al. also define three level of abstraction:

- 1) At the first level, DFMA offers concrete tools, techniques, and guidelines to adapt a design to a given set of downstream constraints.
- 2) At the next level of abstraction, DFMA aims to understand and quantify the effect of the design process on manufacturing (and vice versa).
- 3) At the highest level, DFMA explores the relationship between design and manufacturing and its impact on the designer, the design process, and design practice.

The present thesis work focuses on the second level of abstraction for 3D printed composites. The experimental setups tried to quantify the effects of some design parameters in the final mechanical properties. From this analysis, some guidelines were presented, contributing to the first level of abstraction.

Klahn et al. [35] present two design strategies to use AM benefits in product development: a manufacturing-driven design and a function-driven design strategy.

- 1) The manufacturing-driven design strategy uses AM as a production technology. This strategy requires a designer to comply with the design rules of conventional manufacturing, and when the product is established in the market and sales increase, the production can easily be transferred to a different manufacturing process. This approach is still not attractive for the industry due to small printing envelopes and limited speed of the process. The expensive equipment, high material costs and larger post-processing times are also obstacles in this approach.
- 2) The function-driven design strategy exploits the characteristics of AM to improve the functions of a product. The designer neglects all conventional design rules and designs the part only according to the functions of the component, and the constraints of the AM process.

The present thesis work focuses on the function-driven design strategy for 3D printed composites. The 3D printed components in the two cases of application were designed following the design guidelines found, and oriented to fully exploit the benefits of AM.

One of the trends of function driven strategy is the introduction of lattice cell. Tao and Leu [36] provide a complete review and discussion of AM processes, design methods and considerations, mechanical behavior, and applications for lattice structures. They conclude that the lattice structures have demonstrated excellent architectural, mechanical and functional flexibilities. The AM lattice structure goes beyond the boundary between material and structure. These geometries can integrate more than one function into a physical part, providing practical solutions to a wide range of applications. Figure 4 show examples of lattice structures fabricated by different AM processes: (a) FDM, (b) SLA, (c) SLS, (d) SLM, (e) EBM, and (f) FEF.

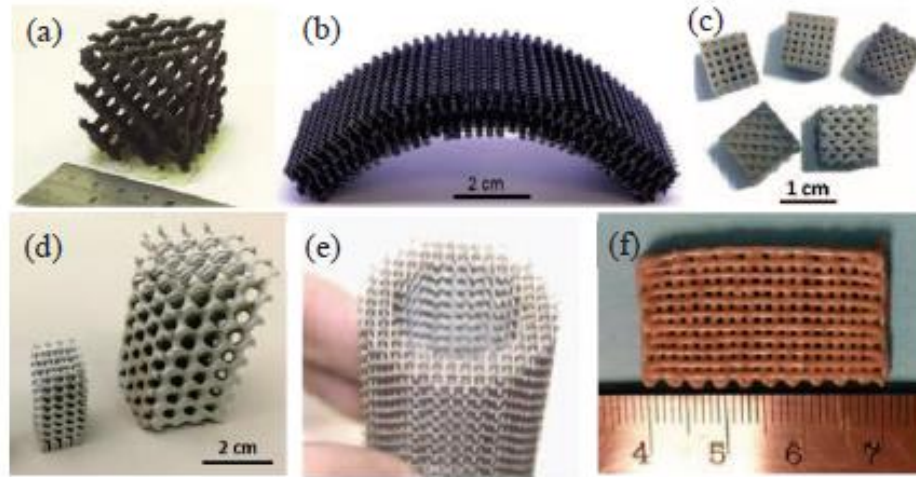


Figure 4. Examples of AM lattice cells. Taken from [36]

Klahn et al. [35] conclude that the challenge of the designers is to use the unique characteristics of AM in the development process to create an added value for the manufacturer and the user of a product. Some of the benefits of use DFAM in the developed process are: improve the performance of the AM manufacturing system, the optimization of fabrication process (cost, functionality, customer satisfaction, etc.) and the evolution of product quality. For example, Klahn presented some cases for SLS and SLM that shows how the re-design for Additive Manufacturing contributed to the success of the product, improving its technological and economic viability.

In the field of 3D printed FRC composites, Brooks and Molony [37] propose a design methodology to integrate continuous reinforcement into AM polymer matrix with the aim of improving their mechanical properties. The method proposes to reinforce with fiber all areas of high Von Mises stress. The fiber strands must be aligned with the first or second principal stresses. The method is validated with the design and testing of three case studies: 1) a pulley housing, 2) hook and 3) universal joint used to demonstrate the applicability for tensile, bending and torsion loading types respectively.

Physical testing showed that it was possible to improve the strength of parts by over 4000%, and stiffness by approximately 200%. The analysis of the specific strength of the parts suggests that the reinforced parts are comparable to aluminum alloys, suggesting

that in some cases AM polymer composite parts could supplant more costly metal parts. Figure 5 summarizes the geometry used in the simulation process, and the final AM parts reported in the article.

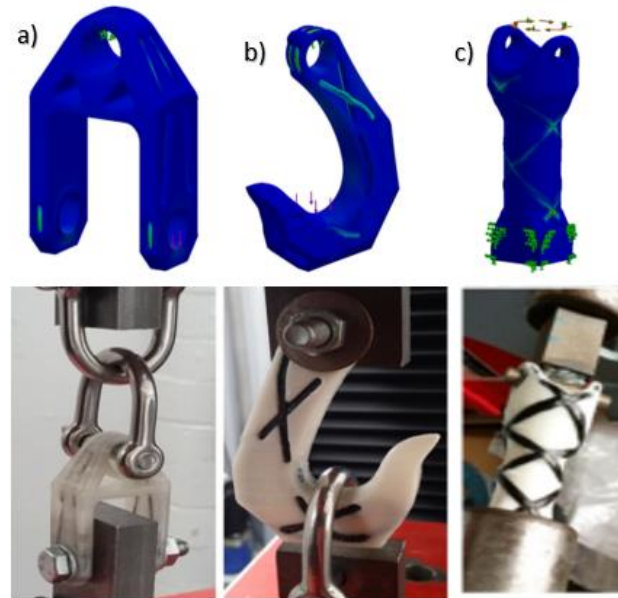


Figure 5. DFAM cases of study simulation and real AM parts from [37]

a) Pulley housing b) Hook and c) Universal Joint

In general, the AM technologies covers a huge range of materials and machines. The final properties of the 3D printed parts are related to several process parameters, including geometric variables. The DFAM strategies in AM cannot be defined with general guidelines. Because of these facts, the DFAM is an open research field that needs to develop specific design rules for specific AM technologies and materials. In this thesis work an evaluation of carbon fiber reinforced composites produced by Fused Filament Fabrication is conducted to contribute with some design guidelines in this field.

Chapter 3: Experimental Setup

This chapter presents the characteristics of the materials tested in the different experimental setups. Two AM fabrication process, chopped (Type 1) and continuous fiber reinforced (CFR) (Type 3) were studied in this work. This section describes the geometric parameters evaluated. The fabrication and characterization equipment used in the three experimental setups are also presented.

In each experimental setup, a mechanical analysis and a fracture mechanism examination are conducted. For mechanical evaluation, several strain-stress tests were performed using three universal tensile machines with different load capacities, while for fracture and morphological analysis, an optical and a scanning electron (SEM) microscopes were used.

3.1 Materials and Fabrication Process

3.1.1. Plastic Matrix

In Fused Filament Fabrication (FFF), the printer heats the thermoplastic filament to near melting point and extrudes it through its nozzle, building a plastic matrix layer by layer. Markforged prints Nylon (Figure 6a.) and Onyx (Figure 6b.) by this method. The filaments are produced with a diameter of 1.75 mm. The polymer must be stored in a moisture-sealed modified dry box to prevent deterioration of the matrix material due to water absorption during storage. [38]

3.1.2. Fiber reinforcement

Markforged parts are primarily composed of plastic matrix. Users may add one type of fiber reinforcement in each part, enhancing its material properties (Figure 6c.). Users can control the layers reinforced, amount, orientation, and reinforcing fiber material. The available reinforced fibers are Carbon Fiber, Kevlar, Fiberglass, High-Strength High-Temperature Fiberglass [38]. The reinforcing carbon fiber (CF) filament is supplied with a diameter of 0.35 mm. The filament is composed of fiber bundles infused with a sizing agent. The individual fiber diameters within these bundles could contain up to 1000 fibers, as reported in [8].

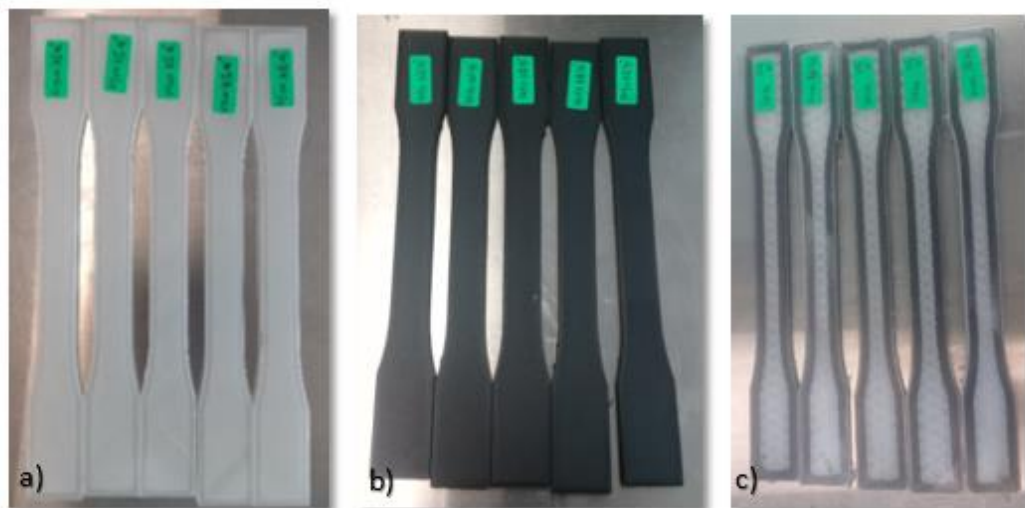


Figure 6. 3D Printed Specimens for a) Nylon b) Onyx and c) CFR (carbon fiber) composite made by Marktwo

3.1.3. Fabrication process

The fabrication equipment is a Marktwo printer. This AM system has a dual extrusion head to allow manufacturing 3D printed parts with Onyx filament (Type 1) and continuous filament fabrication (Type 3). Figure 7 shows the different types of specimens that can be printed with a Marktwo printer.

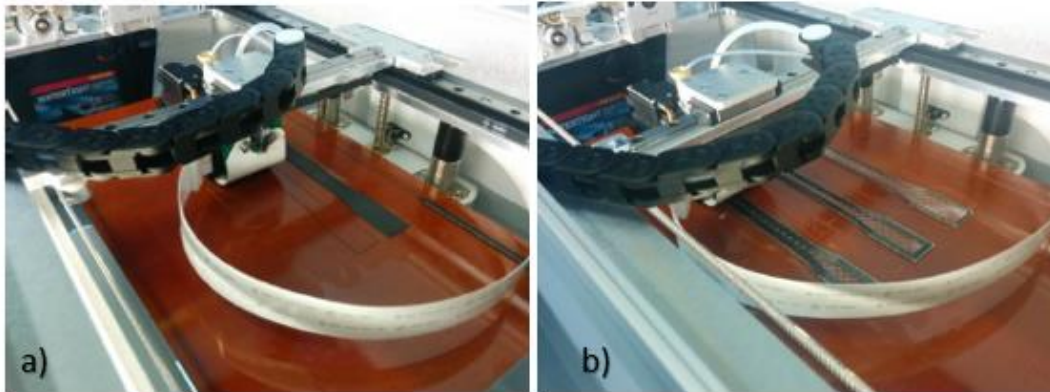
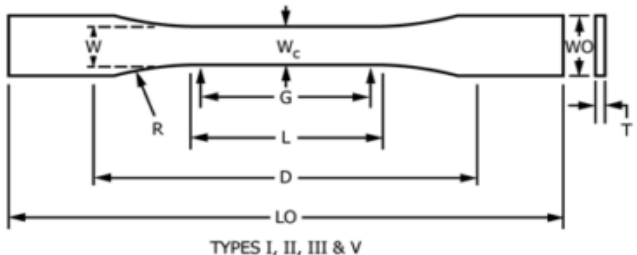


Figure 7. Fabrication of a) Onyx samples (Type 1 fiber embedding method) and
b) CFR composites (Type 3 fiber embedding method)

Five samples for each case built. The test specimen geometry was created using a computer-aided design (CAD) software package (SolidWorks 2016). The CAD geometry of the specimens was exported as a stereolithography file (STL) and loaded into a cloud slicing software (Eiger 2017) package.

Test specimens were fabricated following ASTM D638 Standard Test Method for Tensile Properties of Plastic. The standard specifies that for reinforced composites, including highly orthotropic laminates, the samples shall conform to the dimensions of Type I [39] . The geometry and dimensions are reported in Table 6.

Table 6. Specimen Dimensions for Type I geometry ASTM D638-14

Sample geometry variable	Value	Type I geometry
Length (L)-mm	57	
Width (W)-mm	13	
Thickness (T)-mm	3.2	
Overall length (Lo)-mm	165	
Overall Width (Wo)-mm	19	
Gage length (G)-mm	50	
Distance grips (D)-mm	115	
Radius of fillet (R)-grades	76	

The Tabbing guide [40] for composite test specimens was used to attach cap strips in the samples. The cap strips eliminate the effect of grip force in tensile properties in experimental setup 3. Adhesive and glass fabric/epoxy laminated circuit board was used as tabbing material. The tabs dimensions were made according to recommended tabbing guide. The surfaces were cleaning with isopropyl alcohol, and a special adhesive for the application, 3M Scotch-Weld DP810 was used. Figure 8 shows the materials and the application of cap strips on CFR samples.

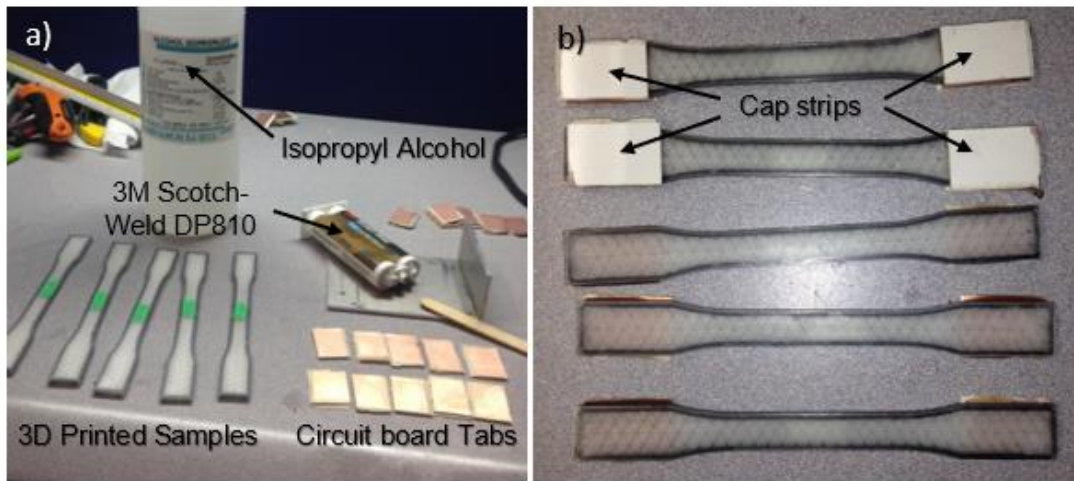


Figure 8. Application of cap strips on CFR samples a) Materials used
b) CFR samples during the process

3.2 Characterization Equipment

3.2.1. Tensile Test Equipment

Most of the tensile tests were performed utilizing an Instron 5KN 3365 tensile machine. Due to the high load capacity required to fracture the specimens with more than 10% of volume fraction reinforcement, a SHIMADZU 100 KN and MTS 810 250KN were also used. The specimens were held in place using wedge clamps and tested at a crosshead speed of 5 mm/minute as per ASTM D638 standard. Figure 9. Shows and Onyx and CFR specimens during the tensile test performed.

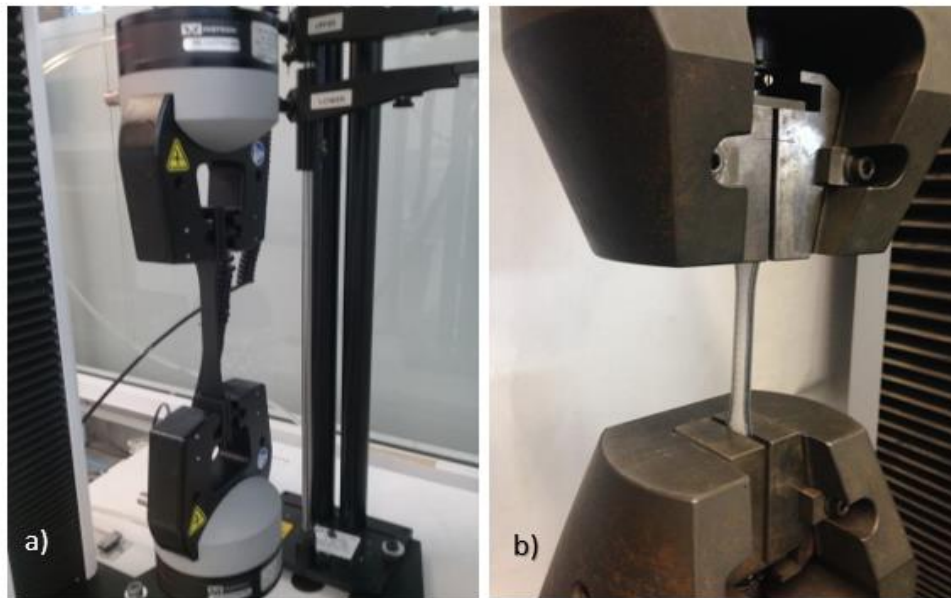


Figure 9. Tensile Test a) Onyx sample on Instron 5KN 3365 and b) CFR composites on SHIMADZU 250 KN

For all the cases, the strain-stress and load-displacement curves were recorded. The Elastic Modulus for each specimen was calculated by software and verified with the raw data.

For Onyx and CFR samples, because of their brittle fracture behavior, the Tensile (Yield) Strength was determined in base of the maximum load found during the tests. For Nylon samples, due to elastic deformation mechanism and test time (more than 90 min

needed to break the specimen), the tests were carried only to a deformation of 25%. Tensile (Yield) Strength was calculated as a ductile material, tracing a parallel to elastic modulus at 0.02 strain, and finding the intersection with the stress-strain curve.

3.2.2. Microscopy Equipment

After the tensile tests, the fractured specimens were examined using Stereo ZEISS optical microscopy for Onyx samples, and SEM EVO MA25 ZEISS microscopy for continuous reinforced samples. Figure 10 shows some samples observed in SEM microscopy.

For SEM microscopy, the samples were extracted from broken specimens, cleaned in an ultrasonic bath (Metason 200) with isopropyl alcohol, and coating with gold in a Quorum Q150R ES equipment. A preliminary procedure was not needed for Stereo optical microscopy.

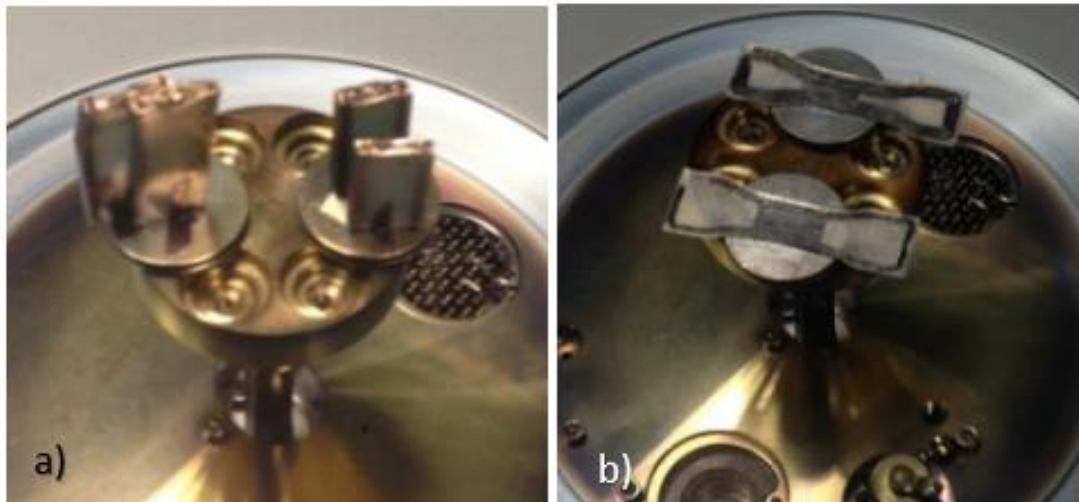


Figure 10. SEM microscopy samples a) Fracture specimens
b) 1R vs. 3R arrangement samples

3.2.3. Composition Equipment

To determine the percentage of carbon fiber in Onyx specimens, a Perkin Elmer Frontier spectrometer was used. For the FTIR analysis, two samples were printed, one wafer of Onyx with a thickness of 0.5 mm and one printing Nylon cord (used as reference) with a thickness of 1.67 mm. The samples were analyzed in Transmission mode following the guide in FT-IR Sample Handling report [41]. The report recommends Transmission mode for Thin Dark Polymer Films. Figure 11 shows the Onyx specimen during the FTIR analysis.



Figure 11. Onyx sample during an FTIR analysis

3.3 Experimental Setup 1: Nylon vs. Chopped Reinforced samples

The objective of this experiment is to determine and analyze the changes on tensile properties due to the matrix material, infill density, and infill geometry for 3D printed parts produced by Fused Filament Fabrication.

For Onyx and Nylon specimens, the infill geometry and density parameters were varied to build a full factorial 2^3 experiment. The following three factors were used:

- Material: Onyx or Nylon,
- Infill Density: 10% and 70 %, and
- Infill Geometry: Rectangular- R45° and Triangular- T0°

The overall printing parameters used to manufacture the test specimen in the two experiments of this study are summarized in Table 7.

Table 7. Printer Parameters defined in Slicing Software

Parameters	Value
Material	Onyx/Nylon
Infill Density %	10%, 70%
Fill Pattern	R45°, T0°
Number of Floor layers	4
Number of Roof layers	4
Number of Wall rings	3
Layer Thickness-mm	0.125

3.4 Experimental Setup 2: Continuous carbon fiber reinforcement samples

The objective of this experiment is to determine and analyze the changes on tensile properties due to fiber volume fraction, and “printing architecture” for continuous carbon fiber reinforcement samples produced by Fused Filament Fabrication.

For the continuous carbon fiber reinforcement samples, a ‘concentric’ fiber pattern that forms annular rings was selected. The number of these rings and also the number of layers to reinforce were varied. Based on these parameters, the volume fraction was increased at different levels, and for 3.61%, 7.21% and 10.82%, a different fiber placement arrangement (#rings -#layers) were manufactured. Table 8 summarizes the cases studied with the different printed architecture selected. For all the eight cases, 10% of infill density and the triangular infill pattern were selected.

Table 8. Printer Parameters defined in Slicing Software


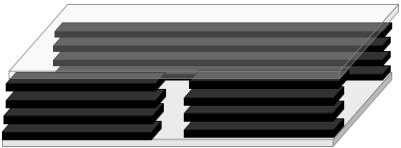

Code	Fiber Rings	Fiber Layers	Calculated Fiber VF	Number of Roof layers	Number of Floor layers	Number of Wall rings
1R-6L	1	6	3.61%	4	4	3
3R-2L	3	2				
1R-12L	1	12	7.21%			
3R-4L	3	4				
1R-18L	1	18	10.82%			
3R-6L	3	6				
3R-18L	3	18	32.45%			
5R-18L	5	18	54.09%			

3.5 Experimental Setup 3: Effect of initial point of reinforcement

The objectives of this experiment are to determine the effect on tensile properties due to the start point position of reinforcement and to analyze how the fracture mechanism change when the start point of reinforcement is moved

In the previous cases for Experimental Setup 1 and 2, the start point was fixed outside the tensile area. In real applications, keep the start point of reinforcement outside the load area is not possible. The effect that has moving the initial point of reinforcement to other areas on the tensile properties is evaluated with two additional cases: Middle and Distributed start points. Additional samples for 1R-12L were manufactured, using the slicing software (Eiger, 2017) the initial point of the reinforcement fibers was modified. Table 9 shows the schematics and configuration used in the cases for experimental Setup 3.

Table 9. Printer Parameters defined in Slicing Software

Reinforced Start Point	Schematic	Fiber Rings	Fiber Layers	Number of Roof layers	Number of Floor layers	Number of Wall rings
Outside		1	12	4	4	3
Middle						
Distributed						

In general, Table 10 summarizes the overall printing parameters for the three different experimental setups used in this thesis work.

Table 10. Experimental Setups and main Printer Parameters

Parameters	Setup 1	Setup 2	Setup 3
Materials	Onyx, Nylon	CFR	CFR
Number of cases	8	8	3
Cases	2 ³ Full factorial	1R-6L vs. 3R-2L 1R-12L vs. 3R-4L 1R-18L vs. 3R-6L 3R-18L and 5R-18L	<i>Initial point of reinforcement:</i> Outside, Middle, Distributed
Infill Density %	10%, 70%	10%	10%
Fill Pattern	Rectangular, Triangular	Triangular	Triangular

Chapter 4: Results & Discussions

This chapter presents the results and discussions of the three experimental setups studied. A complementary method based on the Rule of Mixtures to predict the elastic modulus of the CFR specimens is proposed. This section includes the volume fraction calculations for Onyx and CFR specimens, and summarize the design guidelines found.

The mechanical behavior of the three materials studied in this work is described in Figure 12. 3D printed Nylon has an elastic performance, while Onyx and CFR composites behave in a brittle manner. The strength in CFR structures is considerable higher than Nylon or Onyx samples. Detailed information on how various geometric parameters affect this mechanical behavior is presented in the following sections.

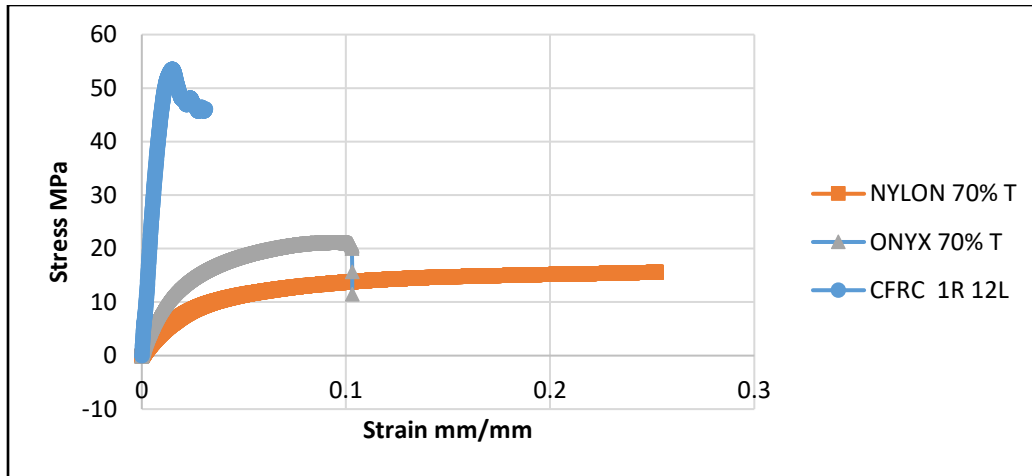


Figure 12. Strain-stress curves for 3d printed Nylon, Onyx and CFR composites.

4.1 Experimental Setup 1: Nylon vs. Chopped Reinforced samples

4.1.1 Tensile Test Results of Experiment Setup 1

Table 11 summarizes the average and standard deviations found for elastic modulus and tensile strength for the eight cases in experimental setup 1. Also, Figures 13 and 14 show a comparison of the results obtained.

Table 11. Results from Tensile Test (ASTM D638) Nylon vs. Onyx Samples

			Elastic Modulus (MPa)		Tensile Strength (MPa)	
Material	Infill Geometry	Infill Density	Mean	St. Dev.	Mean	St. Dev.
Onyx	Rectangular 45°	10%	581.58	86.48	9.80	1.22
		70%	627.31	48.12	11.98	0.59
	Triangular 0°x60°	10%	1064.85	59.72	11.78	0.98
		70%	1293.88	116.08	15.22	0.93
Nylon	Rectangular 45°	10%	311.55	21.03	5.81	0.37
		70%	490.69	34.53	9.55	1.32
	Triangular 0°x60°	10%	358.41	31.21	7.19	0.25
		70%	598.90	14.06	10.43	0.24

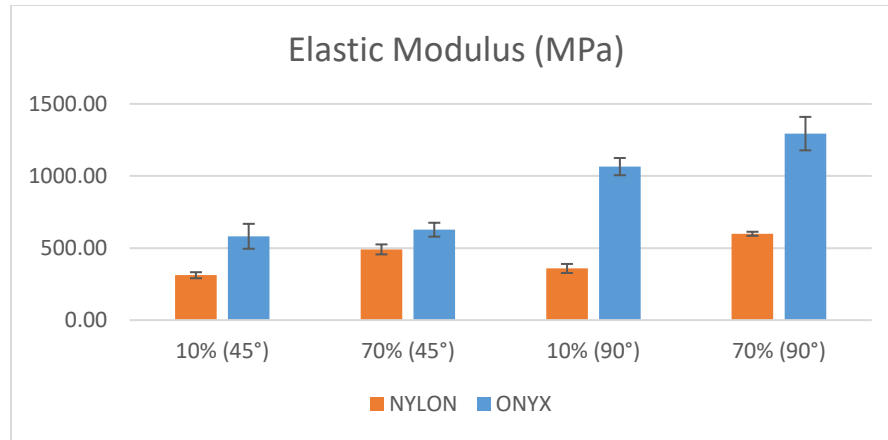


Figure 13. Effect in Elastic Modulus due to material

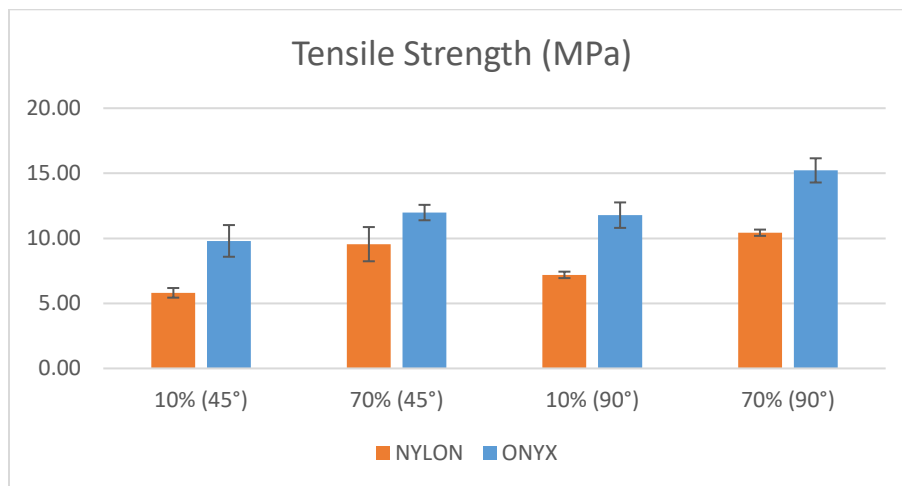


Figure 14. Effect in Tensile Strength due to material

4.1.2 Sensitivity Analysis of Experiment Setup 1

The data obtained in the 2^3 full factorial experiment was analyzed in Minitab 17 through an Analysis of Variance (ANOVA). The results obtained conclude that the differences between the means are statistically significant for the elastic modulus and tensile strength in the three factors analyzed.

General Linear Model: EM versus Material, Infill Percentage, Geometry

Method

Factor coding (-1, 0, +1)

Factor Information

Factor	Type	Levels	Values
Material	Fixed	2	1, 2
Infill Percentage	Fixed	2	10, 70
Geometry	Fixed	2	45, 90

Analysis of Variance

Source	DF	Adj SS	Adj MS	F-Value	P-Value
Material	1	2043216	2043216	527.32	0.000
Infill Percentage	1	301356	301356	77.77	0.000
Geometry	1	1064240	1064240	274.66	0.000
Material*Infill Percentage	1	13115	13115	3.38	0.075
Material*Geometry	1	618486	618486	159.62	0.000
Infill Percentage*Geometry	1	37409	37409	9.65	0.004
Error	33	127866	3875		
Lack-of-Fit	1	9295	9295	2.51	0.123
Pure Error	32	118571	3705		
Total	39	4205689			

Figure 15. ANOVA results for Elastic Modulus

General Linear Model: TS versus Material, Infill Percentage, Geometry

Method

Factor coding (-1, 0, +1)

Factor Information

Factor	Type	Levels	Values
Material	Fixed	2	1, 2
Infill Percentage	Fixed	2	10, 70
Geometry	Fixed	2	45, 90

Analysis of Variance

Source	DF	Adj SS	Adj MS	F-Value	P-Value
Material	1	148.225	148.225	191.77	0.000
Infill Percentage	1	105.625	105.625	136.65	0.000
Geometry	1	31.329	31.329	40.53	0.000
Material*Infill Percentage	1	1.936	1.936	2.50	0.123
Material*Geometry	1	7.056	7.056	9.13	0.005
Infill Percentage*Geometry	1	0.081	0.081	0.10	0.748
Error	33	25.507	0.773		
Lack-of-Fit	1	2.916	2.916	4.13	0.050
Pure Error	32	22.591	0.706		
Total	39	319.759			

Figure 16. ANOVA results for Tensile Strength

Figure 15 summarizes the ANOVA results for elastic modulus, while Figure 16 shows the ANOVA results for tensile strength. The ANOVA study was conducted with a confidence level of 95% and a significance level of $\alpha=0.05$. The significance (p-values less than 0.05) of material (ONYX vs. Nylon), infill density (10% and 70%) and infill geometry (R45° and T0°) were proved in all cases. For the interaction between factors, *material-infill geometry* and *infill geometry- infill density* affects elastic modulus, while only *material-infill geometry* is statistically significant for tensile strength.

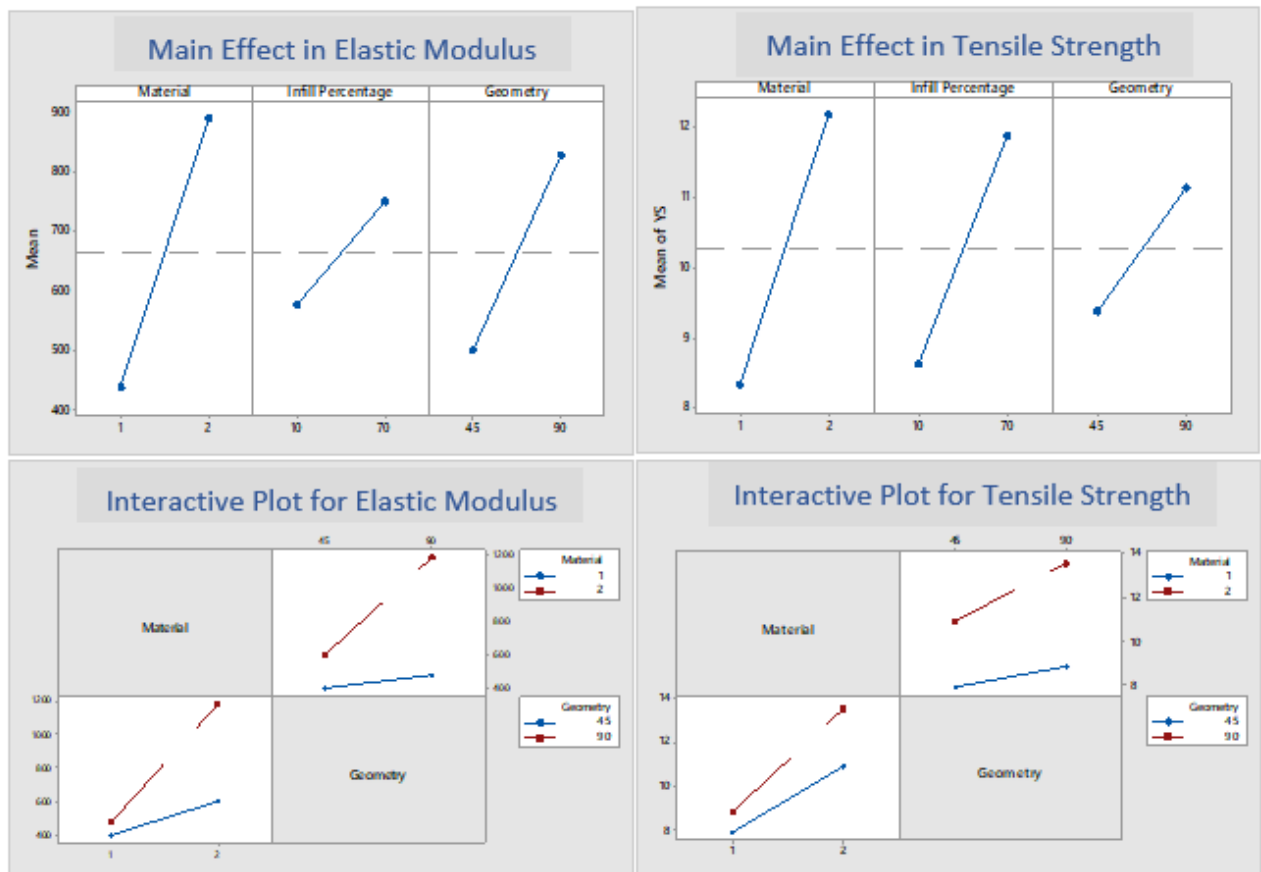


Figure 17. ANOVA factorial plots for Experimental Setup 1

The factorial plots in Figure 17 confirm the interaction between the *material-infill geometry*. It is evident that for both, the elastic modulus and the tensile strength, the infill geometry has a higher effect in Onyx (Material 2) than in Nylon (Material 1). This behavior is likely due to the chopped reinforcement fibers in Onyx. Also, the factorial plots show

that for all the cases, the Triangular pattern ($T0^\circ$) has a better tensile performance than the Rectangular pattern ($R45^\circ$).

In general, the main parameters that affect elastic modulus were material, followed by infill pattern and finally infill density. Regarding to tensile strength, the material is still the main factor, but the infill density has a higher effect than the infill pattern.

4.1.3 Meso-structure Onyx Samples

According to several research groups [42] [43] [44] [45], the integrity and mechanical properties are directly related to the mesostructure characteristics (i.e., the void geometry, the bonding between individual polymer strands, etc.) of fused filament fabricated parts. Since infill density is below 100% in all samples, mechanical properties are determined predominantly by the individual strands.

As seen in the previous section, in Onyx samples the infill geometry has a considerable effect on the mechanical properties. The Triangular pattern shows almost twice the elastic modulus and around 25% more for tensile strength compared with Rectangular pattern. Additional specimens were printed, stopped at layer 13th, and observed in Stereo ZEIS optical microscopy to get a better understanding of how the geometry is constructed. Measurements of the angles were made.

A good congruence with the theoretical orientation angles of 45° for rectangular shape and $0^\circ/60^\circ$ for triangular shape was found. However, the “density” of strands between the two geometries types shows significant differences how can see in Figure 18. The rectangular shape seems to have a higher infill density. This is due to the strands are printed alternately at $+45^\circ$ and -45° . Under these conditions, the contact between the strands will be reduced, while in triangular shape all the strands are stacked in the same orientation. The better contact and the orientation of the stacked strands provide a better mechanical performance.

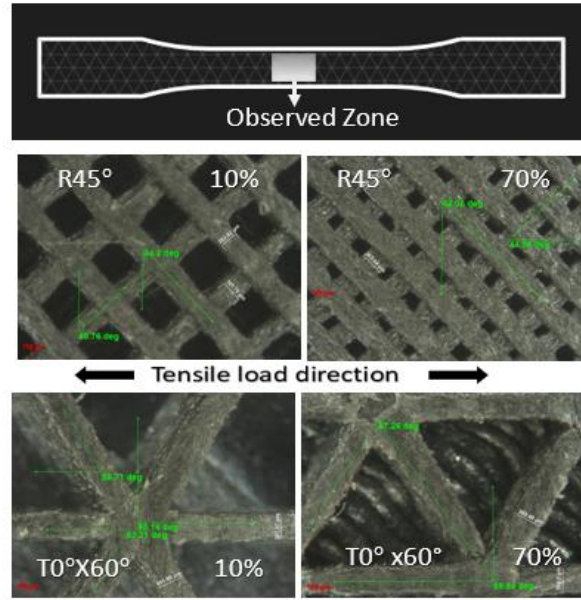


Figure 18. Infill Geometries and Density tested in ONYX samples

4.1.4 Fracture Mechanism for Experiment Setup 1

In Experimental Setup 1 Nylon and Onyx samples were compared. The Nylon samples fail in a macroscopically ductile manner, while Onyx displays brittle failure. For Nylon samples, when one of the strands passes its yield point, exhibits plastic strain behavior, and therefore does not contribute any more to the overall force. As a consequence, the effective area reduces. The neighboring strands also reach their yield point, until the whole sample exhibits plastic strain flow. The sample rapidly starts to elongate until final sample failure. This failure mechanism is shown in Figure 19a, where elongated strands can be detected.

Onyx failure mechanism is somewhat different, due to the chopped carbon fibers. The reinforced material has an increased elastic modulus and immediately breaks right after reaching the yield stress. Failure starts when one of the strands reaches its ultimate stress value. However, in this case, the strand immediately breaks, causing an increased stress concentration in the neighboring strands and their subsequent failure. An overall macroscopic brittle failure is the result. Figure 19b shows this brittle failure mechanism in a surface layer of an Onyx sample.

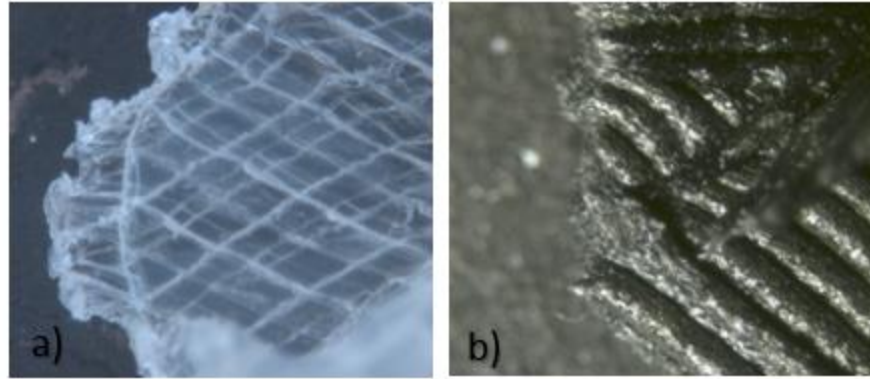


Figure 19. Close-up of failure mechanism of a) Nylon specimen; b) Onyx sample

4.2 Experimental Setup 2: Continuous Carbon fiber reinforced samples

4.2.1 Tensile Test Results Experimental Setup 2

Table 12. summarizes the average and standard deviations found for elastic modulus and tensile strength for the eight cases in experimental setup 2. To test 1R-18L and 3R-6L specimens a SHIMADZU 100KN was used. Due to the high load capacity required to fracture the specimens, 3R-18L and 5R-18L samples were tested on an MTS 810 testing machine. Figure 20 and 21 show the effects of reinforcement volume fraction on the tensile properties of the specimen.

Table 12. Results from Tensile Test (ASTM D638) for CFR samples

Case	Fiber VF	Elastic Modulus (MPa)		Tensile Strength (MPa)	
		Mean	St. Dev.	Mean	St. Dev.
1R-6L	3.6%	2151.98	148.35	27.16	2.37
3R-2L		2295.38	96.77	29.70	1.21
1R-12L	7.2%	3988.91	311.15	51.81	3.89
3R-4L		4471.41	335.45	52.70	2.84
1R-18L*	10.8%	5830.23	390.22	63.20	5.68
3R-6L *		6197.35	361.80	83.72	6.64
3R-18L**	32.5%	10348.60	139.28	151.09	10.11
5R-18L**	54.1%	23690.61	1859.38	304.28	10.19

*Shimadzu 100 KN **MTS810 250 KN

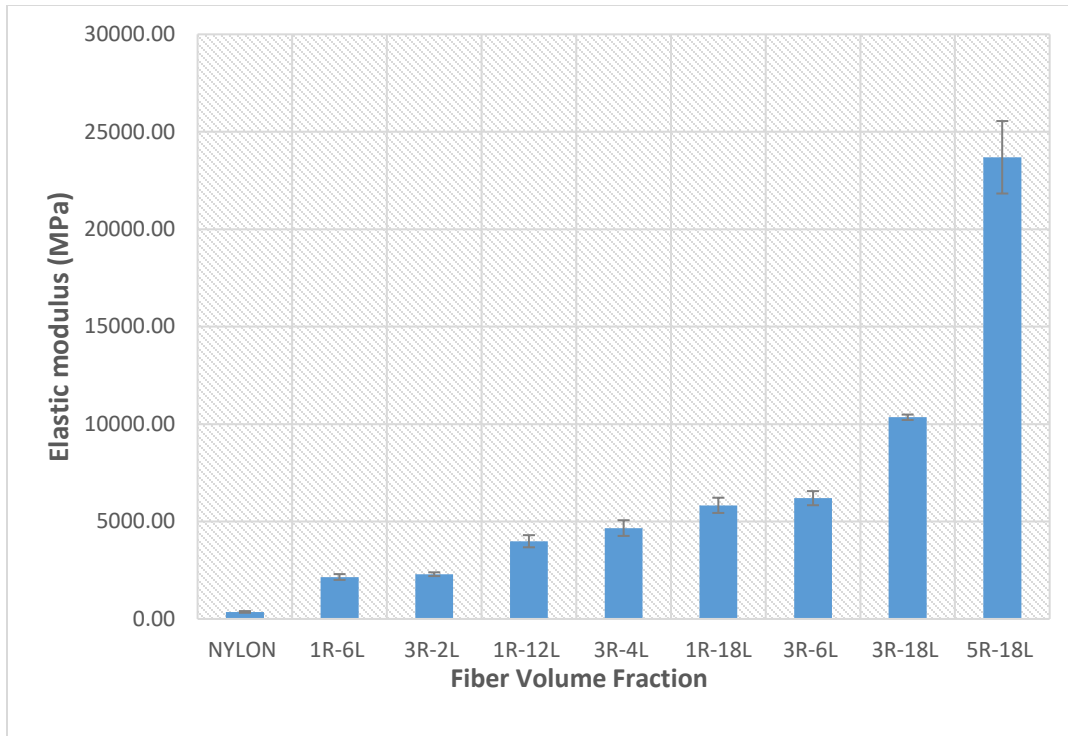


Figure 20. Effect in Elastic Module with respect to Fiber Volume Fraction

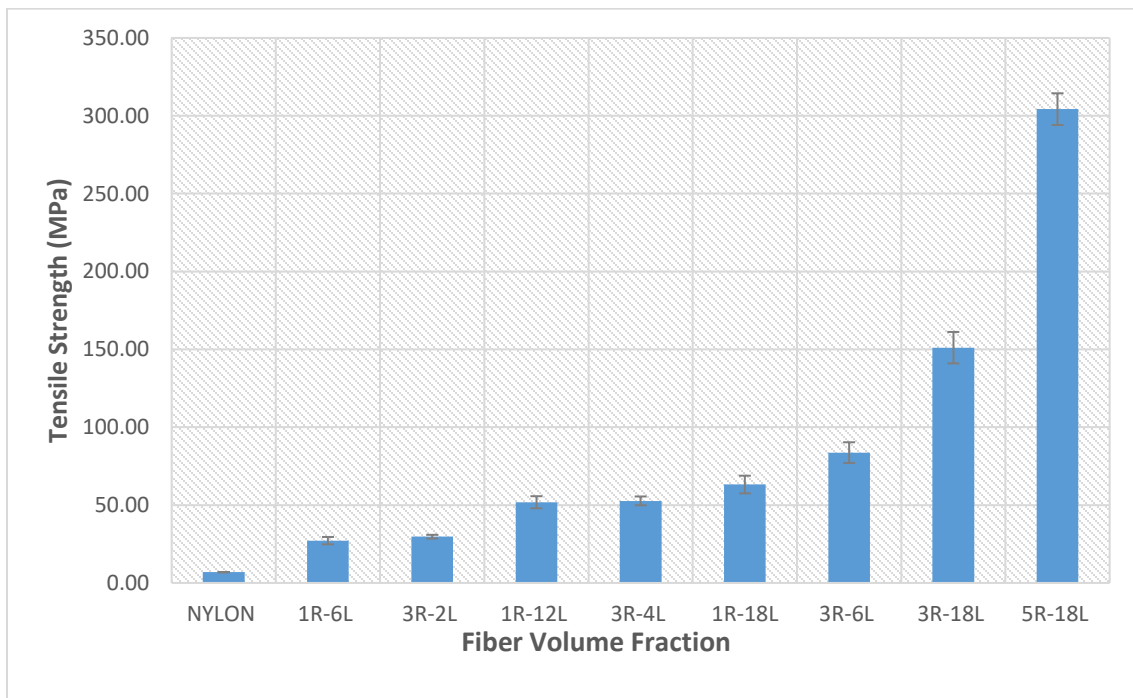


Figure 21. Effect in Tensile Strength with respect to Fiber Volume Fraction

4.2.2 Discussion Experimental Setup 2

The tensile properties obtained for continuous carbon fiber reinforced composite looks promising. The increase in the elastic modulus can go up to 25 times that of E_{nylon} (Nylon Markforged 940 Mpa). In contrast, chopped 3D printed composites (Onyx) shows just small changes in tensile properties. For Onyx samples the elastic modulus can go from 1.2 times that of E_{nylon} (10% R45°) up to 3 times that of E_{nylon} (70% T0°) compared with Nylon specimens with the same printed parameters. For the highest fiber volume fraction specimens tested, 5R-18L, a elastic modulus of 23.7 GPa and tensile strength of 304.28 Mpa were calculated, which is close to the tensile strength (310 Mpa) reported for Aluminium 6061-T6 [46].

Figure 22 and Figure 23 shows a comparison of the samples configuration with the same volume fraction tested in experimental Setup 2. The results suggest that the arrangement of fibers affect the two tensile properties analyzed. A slightly better performance was found for 3R compared with 1R.

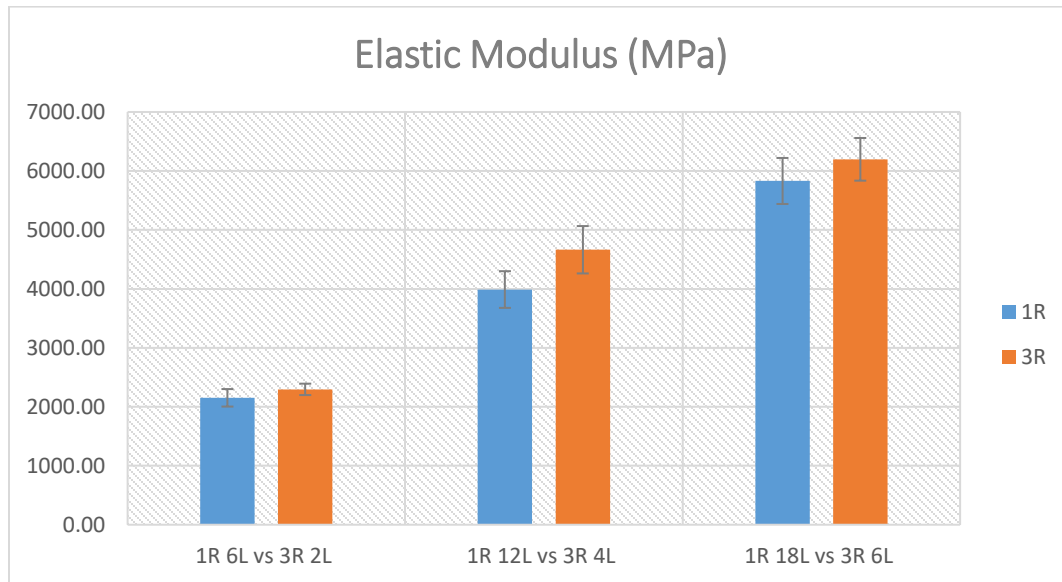


Figure 22. Effect in Elastic Module with respect to sample configuration

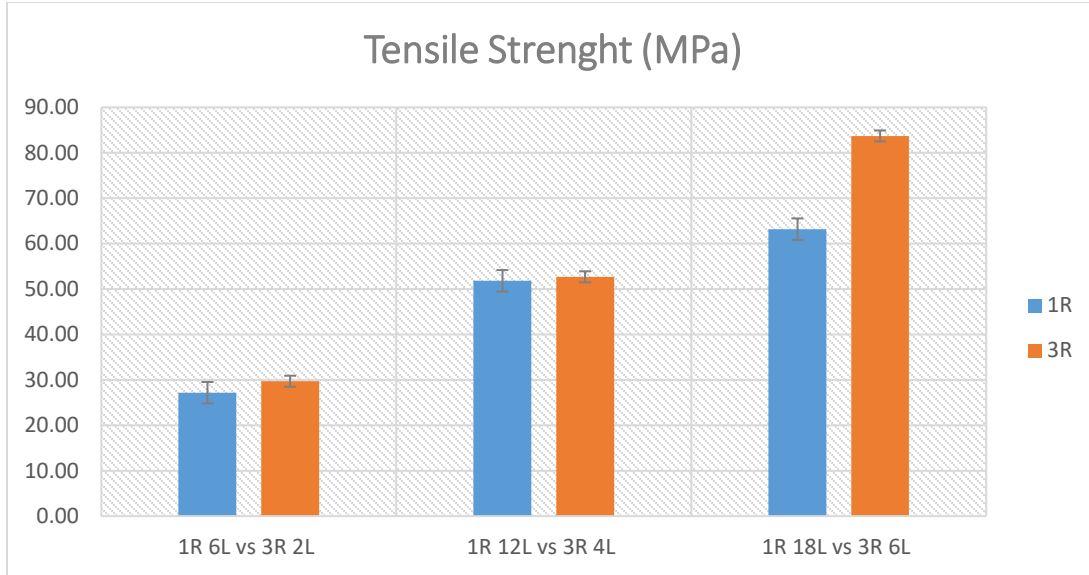


Figure 23. Effect in Tensile Strength with respect to sample configuration

The difference is probably due to the AM process. FDM is a layer by layer procedure. When 3R samples are manufacturing, the fiber rings are printed in the same pass, producing that the fiber rings still have a high temperature to fuse in a single strand as can see in Figure 24b. In contrast, 1R rings are printed at different passes, producing that each fiber rings solidify and acting as stacked separated strands (Figure 24a).

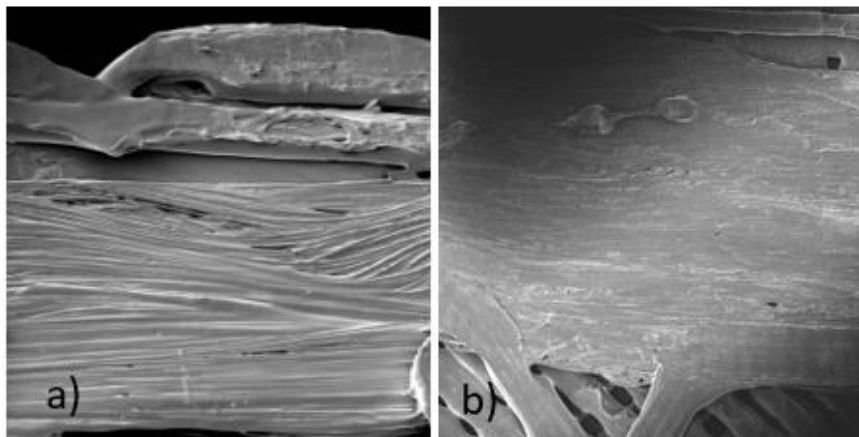


Figure 24. a) 1R layer top view b) 3R layer top view from SEM microscopy

4.2.3 Meso-structure CFR Samples

For continuous CFR composites, the mechanical properties increased considerably by adding higher volume fraction of reinforcement fiber as was presented in Section 4.2.1. However, the variability of the data (Table 12) is high compared with the traditional composite process. This variability could be due to the irregularities in the application of carbon fibers on the prints. The fiber carbon concentric rings have irregularities in the width of strands, as can be seen in Figure 25 and Figure 26. Better control of the toolpath parameters of the fiber could offer fewer deviations in final properties.

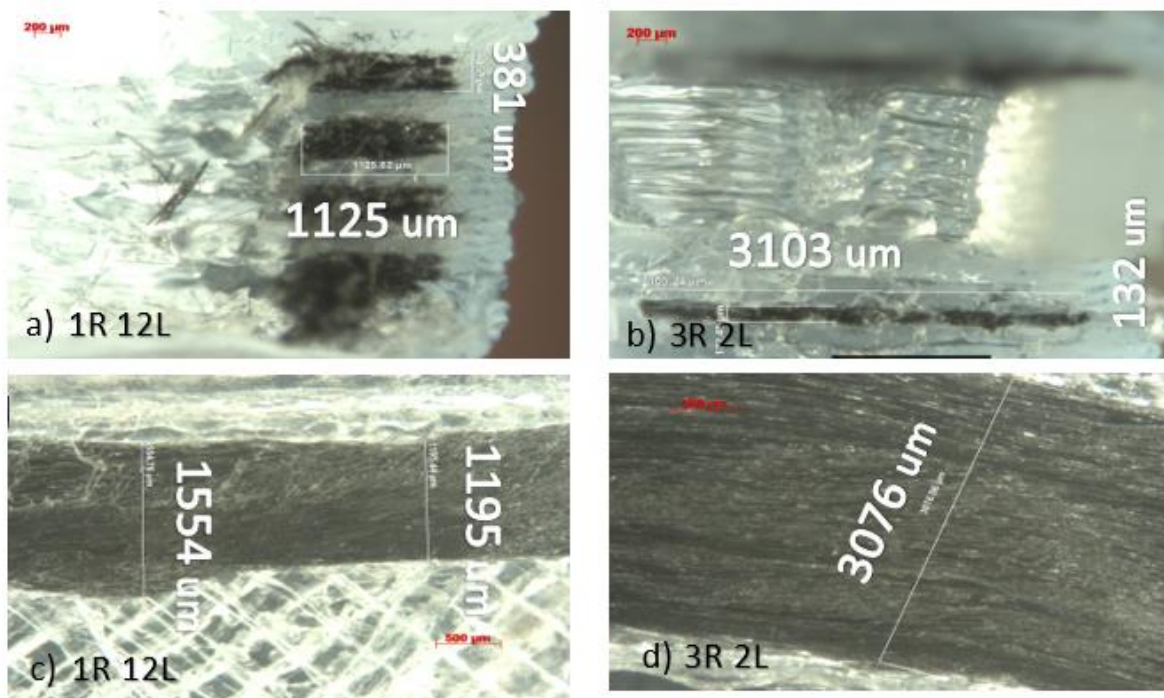


Figure 25. Measured from Stereo ZEIS optical microscopy a) 1R-12L cross view, b) 1R-12L top view, c) 3R-2L cross view and d) 3R-2L top view

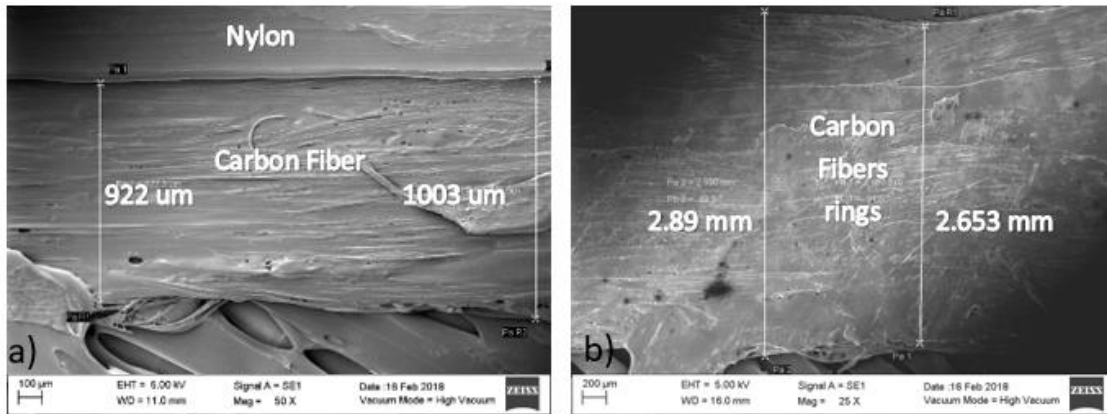


Figure 26. Measurements from SEM microscope at
a) 1R layer top view b) 3R layer top view

4.2.4 Fracture Mechanism Analysis for Experimental Setup 2

Similar to the Onyx samples, the failure mechanism of the continuous carbon fiber reinforced samples also shows macroscopically brittle failure. The continuous bundles of carbon fibers have a limited maximum elongation compared with Nylon matrix. The carbon fiber strands are responsible for withstanding the forces exposed to the samples. When these fiber bundles reach their maximum stress, they break and cause a sudden increase in the stress of the neighboring Nylon strands far above the stresses these Nylon strands can withstand. The sudden increase in Nylon strands exhibits a limited plastic strain flow, resulting in a macroscopically brittle failure behavior. An image of a broken carbon fiber bundle and its neighboring Nylon strand is shown in Figure 27.

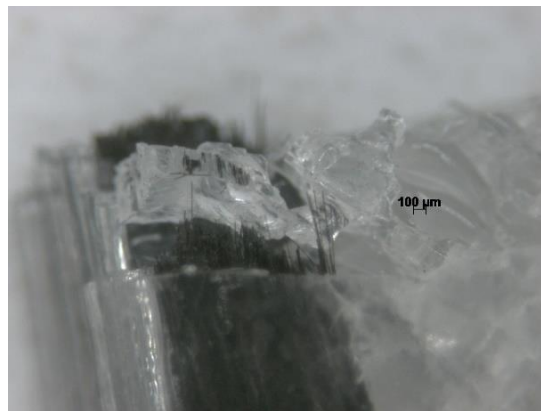


Figure 27. Close-up of failure mechanism of continuous carbon fiber reinforced sample

4.3 Experimental Setup 3: Effect of initial point of reinforcement

4.3.1 Tensile Test Results

In the eight cases for the second setup, with the fiber deposition start point at the tip of the samples (Outside case), most of the specimens fractured in the same area: inflection point in the dog bone as can see in Figure 28. Previous studies by Dickson et al. [27] suggested that the crack initiation coincides with this region due to shear forces experienced by the offset fiber alignment, and through FEM simulations demonstrates the locations of the highest 3rd principal stresses (regions of highest compression) in these points. In contrast, Melenka et al. [28] argue that the break is a product of the starting point of fiber reinforcement.



Figure 28. Break zones in the specimens 1R-12L

The phenomena that produce the failure in CFR composites was analyzed in the third experimental setup. The schematics of the different cases are shown in Figure 29.

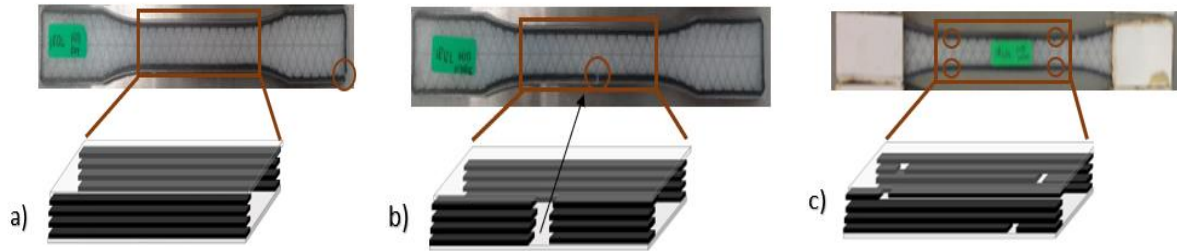


Figure 29. Specimens and schematics of 1R-12L with different start points at
a) Outside (Tip), b) Middle c) Distributed over the tensile area.

Table 13 also summarizes the values for elastic modulus and the maximum strength of the three cases. In the Distributed case the best mechanical properties are obtained, while in the Middle case the worst performance is observed. Small deviations are noticed in the elastic modulus. However, in the maximum strength, the change in this property due to reinforcement start point is more critical.

Table 13. Results from Tensile Test (ASTM D638) for Experimental Setup 3

Case	Fiber Reinforced start point	Elastic Modulus (MPa)		Tensile Stress (MPa)	
		Mean	St. Dev.	Mean	St. Dev.
1R-12L	Distributed	4325.72	79.46	57.66	3.41
	Outside	3988.91	311.15	51.81	3.89
	Middle	3314.65	193.37	43.26	2.55

4.3.2 Fracture Mechanism Analysis for Experimental Setup 3

Figure 30 shows details about fracture mechanism when the start of reinforcement is outside the tensile area. In Nylon material (Figure. 30a) and individual carbon fibers (Figure. 30d), brittle fractures are noticed, while the carbon fiber bundles break in an explosive manner (Figure. 30c).

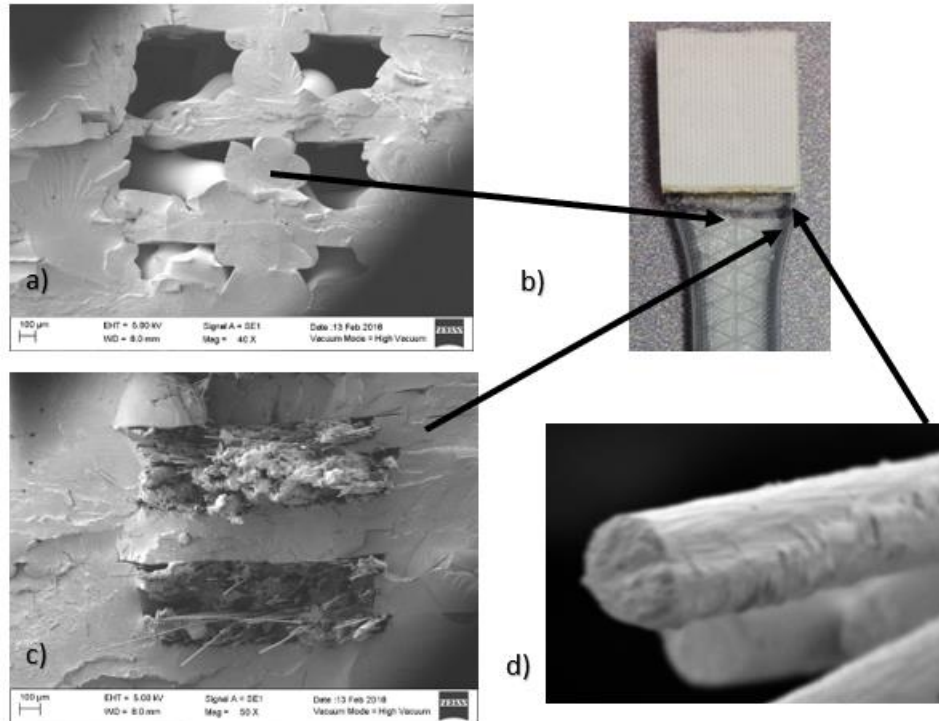


Figure 30. Outside Fracture mechanism a) Nylon area section b) Specimen fractured c) Single carbon fiber, d) Fiber reinforced area section.

In the case when the start of reinforcement is in the middle of the dog bone, the fracture mechanism differs from the side of starting point to side of the continuous fiber reinforcement. The fracture inside of starting point shows that the Nylon material (Figure 31b) breaks elastically, while carbon fiber bundles (Figure 31a) just slipping and delamination from nylon layers. Like the previous fracture mechanism, on the continuous side, the carbon fiber bundles break in an explosive manner (Figure 31d).

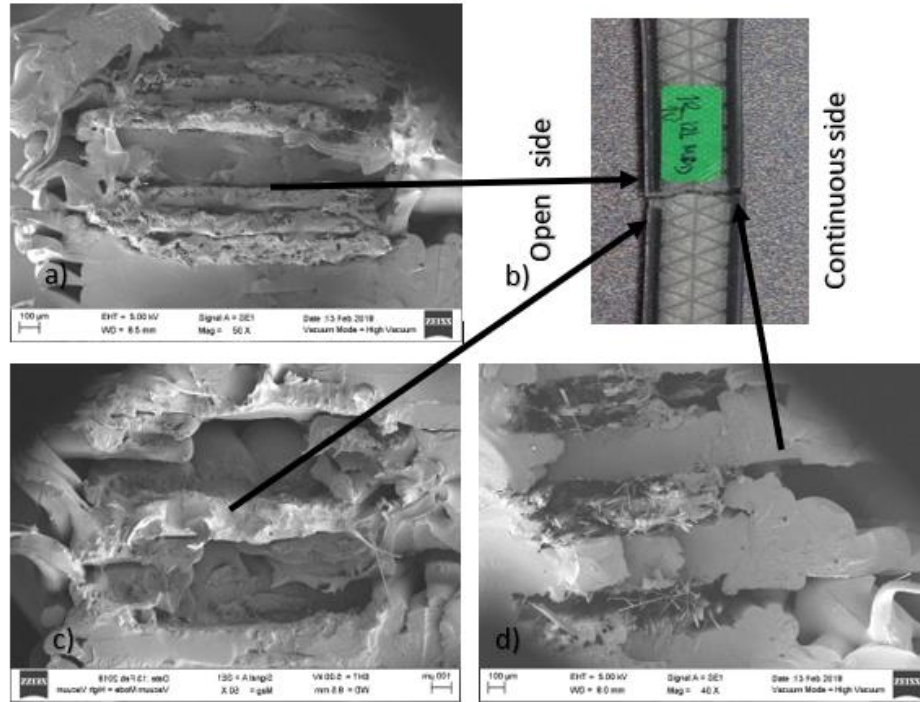


Figure 31. Inside Fracture mechanism a) Start point of fiber bundles b) Specimen fractured c) Opposite view Start of fiber bundles, d) Continuous fiber-reinforced section.

4.3.3 Discussion Experimental Setup 3

These different fracture mechanisms influence the final tensile properties and must be considered as a critical design parameter. The Middle case of 1R-12L compared with the Outside case (regular case) exhibit a decrease of 16.9% in the elastic modulus and 16.5% in the tensile strength. To overcome this reduction in mechanical properties, the case with distributed start points (Figure 29c) over the tensile area was proposed. The Distributed case shows good tensile results. The new samples exhibit an increase of 8.44% in the elastic modulus and 11.29% in the tensile strength compared to Outside case (regular case). This behavior is probably due to the distribution of start points release some compression stresses in the inflection area, preventing the crack initiation in the “outside” fracture mechanism (Figure 30), while the stacked distribution creates only small defects that are not critical for the “inside” mechanism (Figure 31).

4.4 3D Printed Composite Calculations

4.4.1 Composition of Onyx Samples

According to Stuart B. [47], infrared spectroscopy is a technique based on the vibrations of the atoms of a molecule. An infrared spectrum is commonly obtained by passing infrared radiation through a sample and determining what fraction of the incident radiation is absorbed in a particular energy. The energy at which any peak in an absorption spectrum appears corresponds to the frequency of that sample molecule. Through FTIR analysis the elements that compose a polymer could be found. Additionally, a quantitative analysis of concentration of the elements could be complete using Beer-Lambert law.

The Beer-Lambert law is used to relate the amount of light transmitted by a sample to the thickness of the sample. The absorbance of a solution is directly proportional to the thickness and the concentration of the sample [47], as follows:

$$A = \epsilon * C * l \quad (1)$$

Where **A** is the absorbance of the solution, **C** the concentration, and **l** the path length of the sample. The constant of proportionality is usually given the epsilon, ϵ , and is referred to as the molar absorptivity. Additionally, the absorbance is related to Transmittance (**T**) as follows:

$$A = -\log T \quad (2)$$

Onyx is a material registered by Markforged with an unknown percentage of reinforcement. Onyx is a composite filament that contains chopped carbon fiber in a Nylon matrix. In this section, a Fourier Transform Infrared (FTIR) analysis is proposed to find the composition and detail information of Onyx samples in experimental setup 1. The results obtained are summarized in Figure 32.

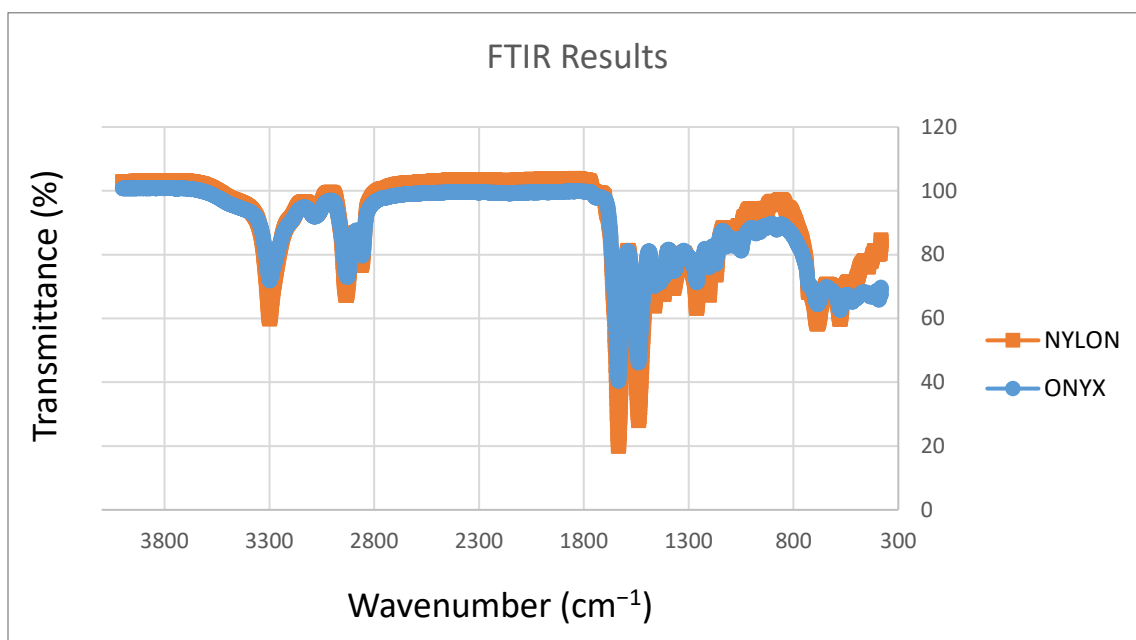


Figure 32. FTIR spectrums for Nylon and Onyx samples

From a preliminary inspection, the spectrums of Onyx and Nylon looks similar. Almost all the peaks in Onyx spectrum shows lower transmittance than Nylon; this behavior is related to the difference in thickness of the samples. However, in the zones of 1000-1100 and 350-550, the Onyx shows higher transmittance than Nylon.

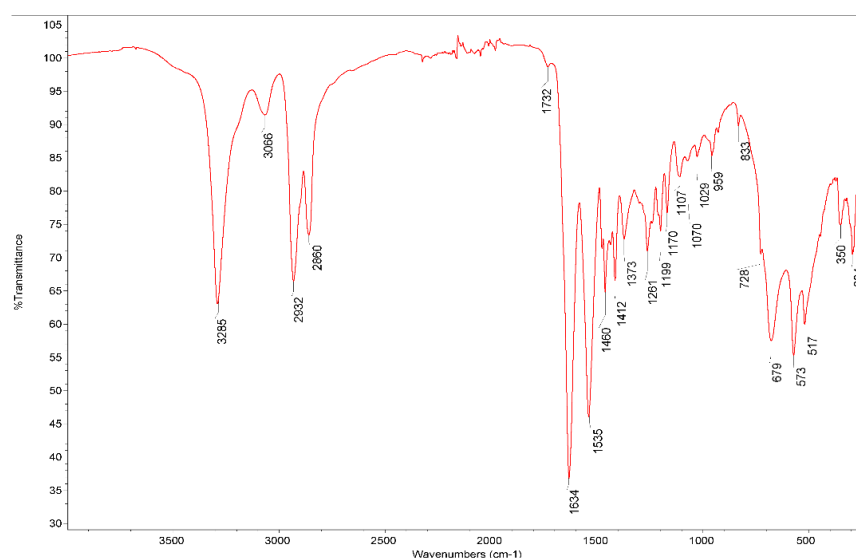


Figure 33. FTIR spectrum for Polyamide (Nylon 6). [48].

Several FTIR spectrums were examined in a database of ATR-FT-IR spectra of various materials [48]. The most similar spectrum of Nylon and Onyx samples was the FTIR spectrum of Polyamide (Nylon 6) as can see in Figure 33. For carbon fiber material any FTIR spectrum was found.

According to Freitag et al. [49], the similarity of the crystal structures of turbo-stratic carbon and graphite led us to the assumption that the optical properties of the carbon fibers can be approximated to the properties of graphite. Using this assumption, Freitag et al. use 355, 532 and 1064 cm^{-1} as reference wavelengths for carbon fibers. In the same way, Xu H. et al. [50] used the same reference wavelengths during its study of the absorption behavior of Carbon Fiber Reinforced Polymer in laser processing. This reference peaks coincide with the zones where the Onyx spectrum shows differences with Nylon spectrum.

For concentration calculations, the polymer matrix peaks were extracted using as reference the Nylon 6 spectrum, and carbon fiber reinforcement peaks were fixed at 355, 532 and 1064 cm^{-1} . To calculate the Absorbance (A) the Equation 2 was used, these values were adjusted by dividing to the thickness in each case. To find the absorbance percentage of carbon fiber in Onyx, the sum of the values in the three graphite wavelengths (market with gray) was dividing to the total absorbance. Table 14 summarizes the wavelengths taken for calculations and the result obtained.

Following Equation 1, if the molar absorptivity factors for Nylon and carbon fiber are considered the same, the concentration of chopped carbon fiber in Onyx could be directly related to the percentage of absorbance found (19.86%). This value is congruent with a similar chopped carbon fiber material produced by Dutch filaments. The filament is called Carbon-P and has a 20% carbon fiber reinforced in a PET-G matrix.[51]

Table 14. Results from FTIR spectrum analysis of Onyx

Wavelengths cm-1	T	A	A adjusted
3299	71.89	0.1433	2.810
3084	91.86	0.0369	0.723
2933	73.58	0.1332	2.613
2863	80.7	0.0931	1.826
1635	40.33	0.3944	7.733
1538	46.15	0.3358	6.585
1262	71.28	0.1470	2.883
1064	84.78	0.0717	1.406
685	64.42	0.1910	3.745
576	62.62	0.2033	3.986
532	67.01	0.1739	3.409
380	67.56	0.1703	3.339
Thickness sample (cm)			0.051
Carbon Fiber Absorbance			8.154
Total Absorbance			41.058
Carbon Fiber A %			19.86%

4.4.2 Volume Fraction for CFR Samples

A schematic of the internal structure of the continuous fiber-reinforced 3D printed specimen is shown in Figure 34. Four distinct regions can be distinguished in the test samples: wall region, roof & floor layers, infill layers and reinforced layer. Each region has different mechanical performance due to the printing toolpath. The roof and floor layers region the head follows a path in a range of $\pm 45^\circ$ from the longitudinal axis, while for walls and reinforcement layers the printer toolpath is parallel to the longitudinal axis. Finally, the infill orientation depends on the pattern (rectangular 45° or triangular $0^\circ/60^\circ$) and the density selected.

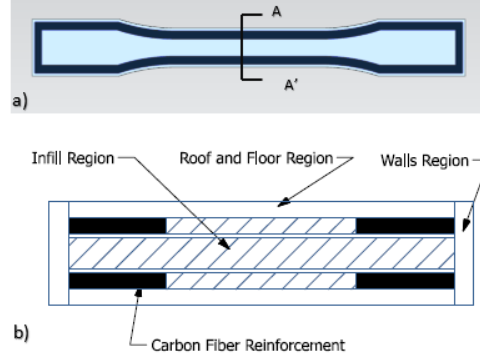


Figure 34. CFR specimen a) Top view b) Cross Section A-A.'

Table 15 summarizes the variable printing parameters (Fiber rings and Fiber layers) in the eight cases for experimental setup 2. The sizes of W_{fiber} and W_{wall} were determined with Stereo ZEIS optical microscopy. The layer thickness is fixed to 0.125 mm by the software. The fiber Volume Fraction (VF) were determined following the procedure reported in [28]. Geometric data were used to calculate the overall tensile volume $V_{composite}$ using Eq. (7), then fiber volume V_{fiber} was estimated using Eq. (6), and finally, the fiber VF ϕ_{fiber} of the different cases is found using Eq. (7).

Table 15. Volume Fraction calculations for Experimental Setup 2

Code	#Concentric Rings	#Layers reinforced	Volume Fraction
1R-6L	1	6	3.61%
3R-2L	3	2	3.61%
1R-12L	1	12	7.21%
3R-4L	3	4	7.21%
1R-18L	1	18	10.82%
3R-6L	3	6	10.82%
3R-18L	3	18	32.45%
5R-18L	5	18	54.09%

4.5 Prediction of Elastic Modulus by Rule of Mixtures

For the prediction of the elastic modulus of a composite, the rule of mixtures (Eq.10) can be used as reported by Dickson et al. [27] and Van Der Klift et all [29]. In this section, an alternate method to predict the elastic modulus is presented. The approach proposed considers all the design variables (number of rings, the floor and roof layers, the density of infill, etc.) studied in this thesis. The method consists in the following four steps:

1. To determine the volume for each of the four regions in this type of composites following the Equations 3 to Equation 6.
2. The overall volume of the specimen is calculated with the Equation 7.
3. The volume fraction of the matrix and reinforcement is determining following Equation 8 and 9.
4. Finally, the elastic modulus is calculated with the raw elastic modulus of matrix and reinforcement materials following Equation 10.

$$V_{\text{roof and floor}} = (W - 2 * N_{\text{wall}} * W_{\text{wall}}) * H * T_{\text{layer}} * (N_{\text{floor}} + N_{\text{roof}}) \quad (3)$$

$$V_{\text{wall}} = 2 * N_{\text{wall}} * W_{\text{wall}} * H * T_{\text{layer}} \quad (4)$$

$$V_{\text{infill}} = (W - 2 * N_{\text{wall}} * W_{\text{wall}}) * H * I * T_{\text{layer}} * (N - N_{\text{floor}} - N_{\text{roof}} - N_{\text{fiber}}) \quad (5)$$

$$V_{\text{fiber}} = 2 * W_{\text{fiber}} * N_{\text{fiber}} * R_{\text{fiber}} * H * T_{\text{layer}} \quad (6)$$

$$V_{\text{composite}} = W * H * T \quad (7)$$

$$\Phi_{\text{matrix}} = \frac{V_{\text{roof and floor}} + V_{\text{wall}} + V_{\text{infill}}}{V_{\text{composite}}} \quad (8)$$

$$\Phi_{\text{fiber}} = \frac{V_{\text{fiber}}}{V_{\text{composite}}} \quad (9)$$

$$E_{\text{predicted}} = \Phi_{\text{matrix}} E_{\text{matrix}} + \Phi_{\text{fiber}} E_{\text{fiber}} \quad (10)$$

Where $E_{\text{predicted}}$ is the expected elastic modulus for the specimen, E_{matrix} , E_{fiber} ,

Φ_{fiber} , Φ_{matrix} is the elastic modulus and volume fraction of fiber and matrix respectively. V_i denotes the volumes of the different regions in the composite and $V_{composite}$ is the overall volume of the specimen, I is the infill density; W , W_{wall} , W_{fiber} , H , T_{layer} and T are geometric parameters of the specimen, and N , N_{walls} , N_{floor} , N_{roof} , N_{fiber} and R_{fiber} are the defined number of layers and rings for walls, roof, floor and reinforcement regions discuss in Section 4.4.2.

The predicted elastic modules were calculated using the values described in Table 15 and the elastic modulus of raw materials values of $E_{matrix} = 940 \text{ MPa}$ and $E_{cf} = 50 \text{ GPa}$ obtained from Markforged materials datasheet [52]. The experimental and predicted elastic modules results are summarized in Table 16.

Table 16. Results from Prediction Model by Rule of Mixtures

Case	Fiber Volume Fraction	Elastic Modulus (MPa)		Error
		Measured	Predicted	
1R-6L	3.6%	2151.98	2224.08	3%
3R-2L		2295.38	2236.73	-3%
1R-12L	7.2%	3988.91	4007.98	0%
3R-4L		4471.41	4033.29	-10%
1R-18L	10.8%	5210.80	5791.88	11%
3R-6L		6197.35	5829.25	-6%
3R-18L	32.5%	10348.60	16609.19	60%
5R-18L	54.1%	23690.61	27426.50	16%

The differences between the measured and predicted values are bellow $\pm 10\%$ when the volume fraction is lower than 11%. However, for the other cases, the approach proposed was less accurate. This behavior is congruent with the values reported by Van Der Klift et al. [29] who also found that at higher volume fraction this kind of composites does not behave according to the rule of mixtures. This is probably due to when the fiber content increases this rule of mixtures approach does not consider the anisotropic nature

of the fiber. In contrast, at lower fiber content the mechanical behavior of the composite is dominated by the matrix (Nylon) being isotropic.

For prediction of elastic modulus in CFR composites Melenka et al. [28] used an orthotropic stiffness matrix, which considers the anisotropic nature of the fiber with good results for larger amount of fiber reinforcement. However, for lower fiber reinforced contents, the method fails to predict the elastic modulus.

The method presented provides a simple way to estimate the expected mechanical performance of CFR composites with fiber contents below 11%. This approach complements the Melenka's method and increases the range of values to predict the elastic modulus for CFR composites.

Chapter 5: Design Guidelines and Recommendations

Composite design is a complex process, when it comes to 3D printing, the constraints increase. The 3D print composite process requires that the fiber depositions is done in a single plane. The design is strictly 2D in nature. To exploit the benefits, the design is restricted to the geometry of the part and how it is arranged on the print platform. In this section, some design guidelines are provided. Additional some recommendations about the manufacturing process of FRC composites are presented. All these findings may help the designer to define the best parameters for the print part and will be helpful for improving the mechanical performance of 3D printed composites.

5.1 Design Guidelines for 3D printed composites

Two Cost vs. Strength charts were calculated to correlate the mechanical and fracture performance with the costs of the different samples. Figure 35 shows the Cost-

Strength regions of the eight cases of Experimental Setup 1. The best relation is for Onyx sample with 70% infill density and Triangular pattern.

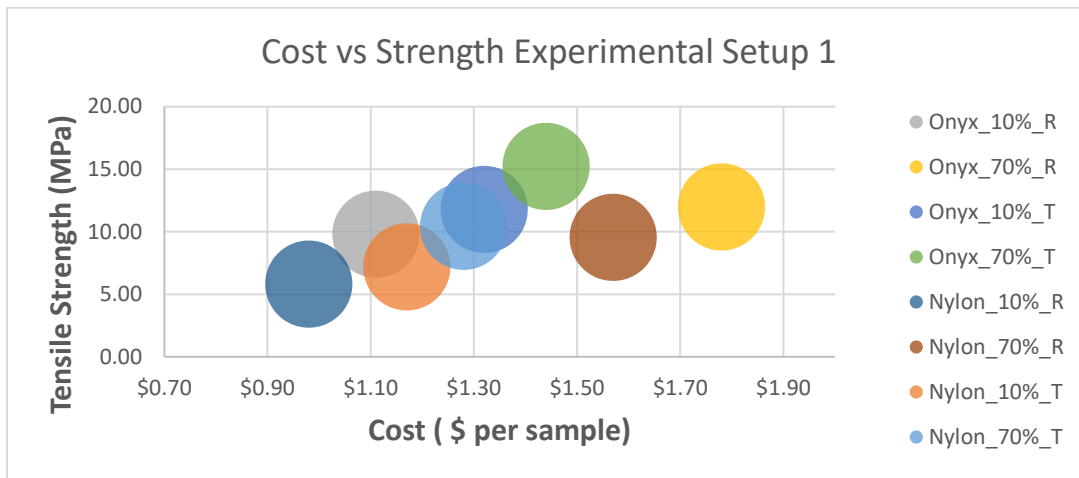


Figure 35. Cost vs. Strength Experimental Setup 1

Figure 36 shows the Cost-Strength regions of the eight cases of Experimental Setup 2 and one Nylon reference case without fiber reinforcement. The relation Cost-Strength is almost linear. The wider arrangements cases show a slightly better Cost-Strength relation, because has the same sample cost.

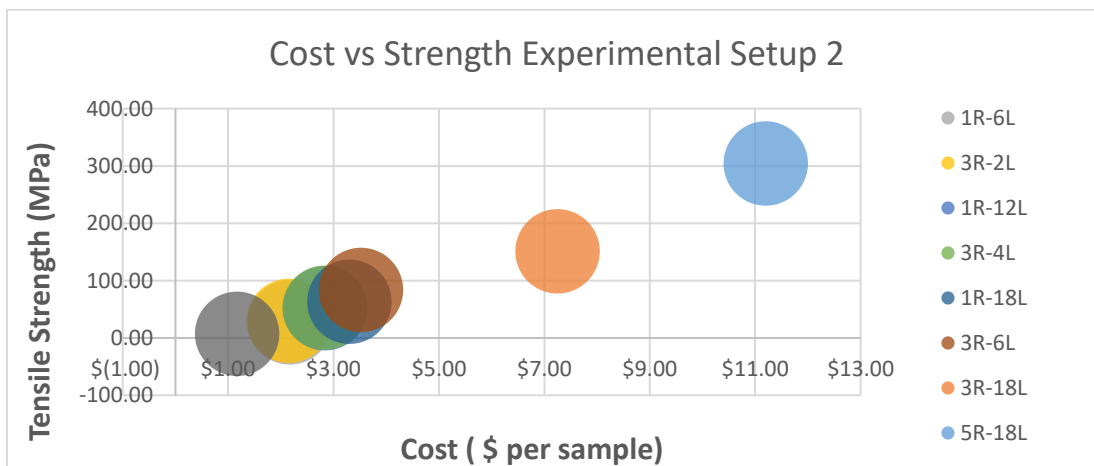


Figure 36. Cost vs. Strength Experimental Setup 2

Material choice

In this thesis work two types of 3D printed composites were evaluated, chopped (Onyx) and continuous fiber carbon reinforced. The first decision for the designer is to define the best material for the application. Different combinations could be printed for CFR composites, Nylon with carbon fiber and Onyx with carbon fiber.

- Onyx (chopped composite) is a good election when the tensile loads are small, the printing time and costs are cheaper than CFR composites.
- For CFR composites, the designer must define the matrix material. The Cost-Strength charts presented in this section must be considered to find the best set of parameters.

Infill density and patterns

For geometric parameters, to improve the mechanical performance of 3D printed composites, the designer must consider:

- Use the triangular fill pattern, especially for chopped composites.
- The infill density has a minor role in the tensile properties. This parameter can be reduced to obtain fewer costs and printing times.

CFR printing architecture

As shown by experimental Setup 2, the printing architecture of the fiber reinforcement affects the final tensile properties.

- Prefer a wider arrangement of the fiber reinforced strands, instead of stacked strands of fiber reinforcement.

Initial point of reinforced

As shown by experimental Setup 3, the start point of reinforcement has an important effect on the final tensile properties.

- The designer must consider the two fracture mechanisms discussed in Section 4.3.2.
- Fixing the initial points of fiber in a distributed manner could prevent premature failure.

5.2 Recommendations

Some printing issues were presented when the Nylon or Onyx filament spools were left in an open environment. Storage the matrix materials in a dry box is a mandatory procedure. Wet material filaments degrade final mechanical properties of the parts.

The variability in the data for tensile results shows that some environmental parameters (humidity, temperature) affects the final properties of the specimens. Monitoring of 3D printing process is recommended. Install some sensors, collect and analyze environmental parameters can help to have a better process control.

For the Experimental Setup 3, the standard deviations of the elastic modulus and tensile strength results were lower than in Experimental Setup 1 and 2. This behavior was due to the use of cap strips in the third setup. For future tests is strongly recommended to add cap strips to the specimens following the tabbing guide reported in Section 3.1.3. The adhesive 3M Scotch-Weld DP810 shows excellent resistance for this application.

Chapter 6: Cases of Application

In this chapter two cases of application that show the benefits of 3D printed composites structures are presented. One is a support structure designed and printing for the upgrading of a quality test equipment. The other is an optimized bracket that forms part of a vision system used in surface defect identification for metal castings. In addition, some recommendations for the manufacturing process of 3D printed composites components.

6.1 Case 1: Mechanical Design for Upgrade Equipment in Industry 4.0 system.

The term Industry 4.0 describes a system that evolved from a computer controlled automated facility (Industry 3.0), into a system that collects, storage and analyzes data from the floor to make intelligent decisions in an automated manner [53]. In Industry 4.0 factories, the control quality equipment goes from being simple checking apparatus to becoming a device that generates information. To accomplish this task, the current manufacturing equipment must be upgraded. The automation of the manufacturing data is the key factor in the fourth industrial revolution.

In this section, the mechanical design and implementation of a support structure made of 3D printed chopped, and CFR composites are presented. The support structure is part of a smart audio system that recorder, storage, and process the data of a quality gear truck test.

According to Ahuett-Garza and Kurfess [54], AM is one of the habilitating technologies that allow implements the Industry 4.0 in the smart factories. AM has the potential to support a wide range of application including manufacturing, special for some specific applications characterized by a high level of customization and low volume production. The support structure of the smart audio system represents an example of the type of specific application where the AM technologies can show its full potential.

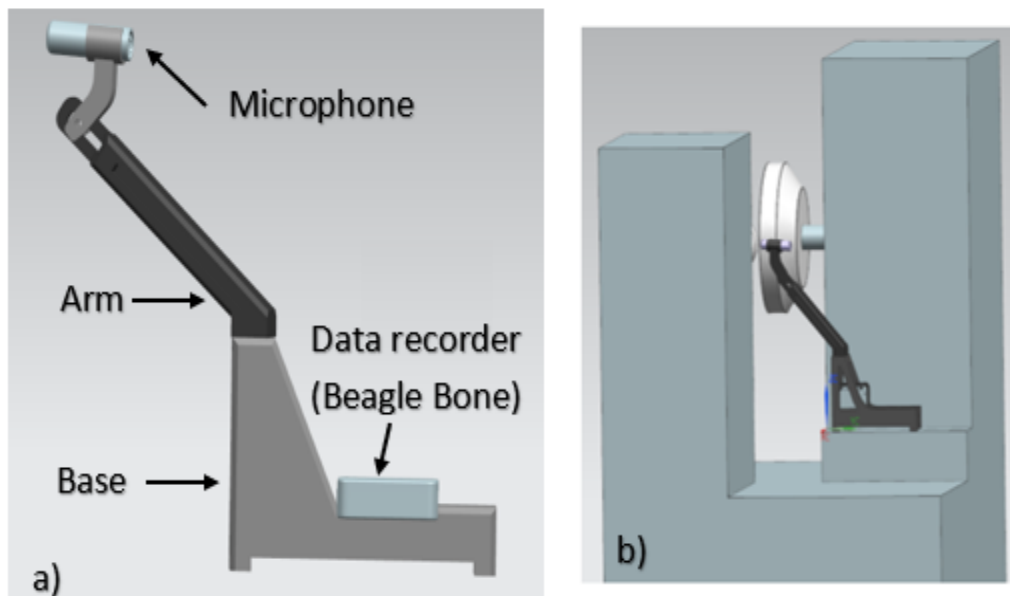


Figure 37. Mechanical design Smart audio system a) Support structure b) Assembly used during design

Figure 37a shows the isometric view of the microphone support built for the smart audio system. The assembly is composed of three parts: arm, pivot, and base. Figure 37b shows the assembly simulation used during the design process. The gray blocks represent the upgraded equipment. Figure 38 present some features incorporate during

the design. The arm and pivots parts were reinforced with carbon fibers that increase the tensile strength of the part. Finally, for an easy and robust mounting design, some magnets were introduced inside the base part during the printing process, something that is complex for any other subtractive process.

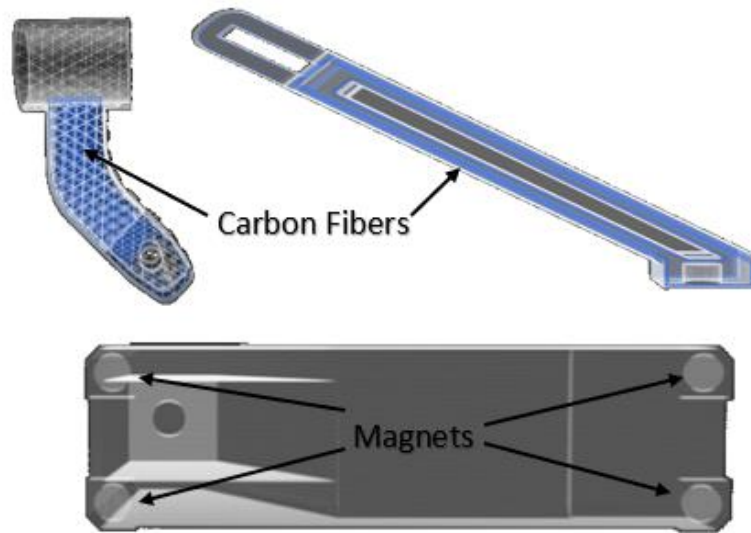


Figure 38 AM composites features incorporated during design.

The support structure was design in NX 10.0 and fabricated with a Marktwo composite 3D printer. Following the design guidelines proposed the next settings were used during the manufacturing process:

- Onyx was used as matrix material, due to the small loads the base was printing without reinforcement. While for the arm and pivot part continuous carbon fibers were used to reinforce the components.
- For all the parts, a Triangular infill pattern and a 25% of infill density were used.
- To reinforce the arm (280 layers) and pivot parts (242 layers), just 8 layers were added with carbon fiber rings. Three concentric rings were added in each layer preferring a wider arrangement.
- The start point of reinforcement was moving by 10% over the 8 layers reinforced, fixing the points in a distributed manner.

A fit analysis following ISO 286-1 for the insertion of the magnets in the print part was conducted. According to Shigley in the Limits and Fits section of his book [55] the recommended tolerance fit for this application will be *Locational clearance fit* (H7/ h6). This selection provides snug fit for location of stationary parts but can be assembled and disassembled. Table 17 shows the calculated tolerances for shaft and hole using the recommended fit H7/ h6. However, for the magnets (shaft) and holes in the base part, the resulted tolerances cannot be achieved its corresponding manufacturing processes. According to Annex 3 the expected tolerance for magnets is $\pm 100 \mu\text{m}$, while for holes in the base part, the tolerance of AM process is the layer thickness ($\pm 125 \mu\text{m}$). Table 17 also shows the values for the real fit (H13/ h12) used in this case of application.

Table 17. Fit analysis results for magnets (shaft) inside the base part

Variable	Recommended Fit		Real Fit	
	Hole	Shaft	Hole	Shaft
Type of Fit	Clearance		Clearance	
Fit	<i>H7/ h6</i>		<i>H13/ h12</i>	
Upper deviation (μm)	18	0	270	0
Lower deviation (μm)	0	-11	0	-180
Maximum size (mm)	12.718	12.7	13.07	12.8
Minimum size (mm)	12.7	12.689	12.8	12.62
Clearance (μm)	± 14.5		± 225	

The overall printing time was 34 h, and the material cost was \$99.87. This case of application verifies the benefits and flexibility that Additive Manufacturing offers for its use in upgrading equipment to Industry 4.0. Figure 39 shows the final printed support structure.

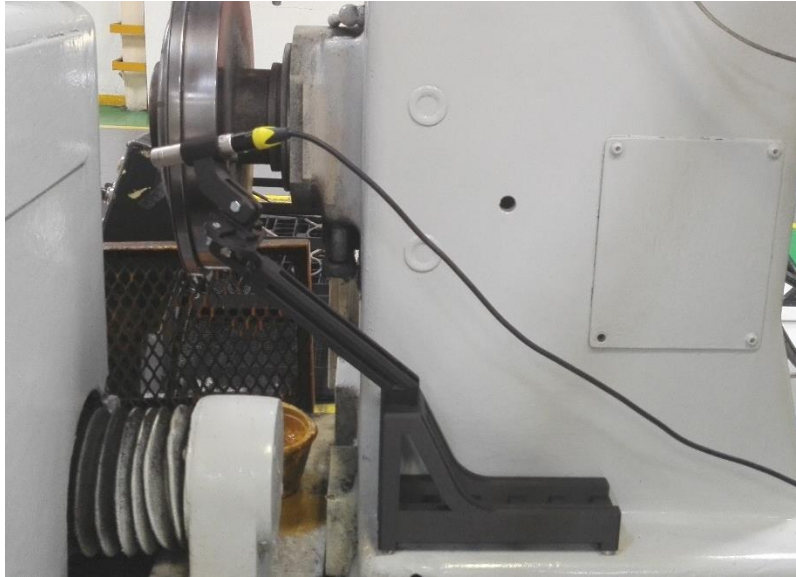


Figure 39. 3D printed support structure for Smart audio system

6.2 Case 2: Topology Optimization of Carbon Fiber Reinforcement Bracket for a Vision System.

The optimized component is a bracket that forms part of a vision system used in surface defect identification for metal castings [56]. Hyperworks was the FEA and topology optimization platform. Hypermesh and Hyperview were used as pre-processor and post-processor software respectively. The solver package was Optistruc. Using the design methodology proposed by Brooks and Molony [37], an exploratory case of study is presented in this section. The design steps of this methodology are the following.

- Define the design space, loads, and constraints.
- Evaluate design with FEA. Determine how the internal forces will be transmitted through the part (Topology Optimization)
- Design the final part. The reinforcement path should go through all areas of high Von Mises stress. The reinforcement path should be continuous with as few discreet loops as possible.
- Manufacturing and physically test.

1. Following the Brooks and Molony method, the design space, loads, and constraints were defined.

Using Hypermesh package, two analyses with different design space geometry were conducted. Figure 40 shows the design, non-design space, the constraints and the loads. The card image material was defined as PSOLID and Orthotropic (MAT 9). The constants used was obtained from [57].

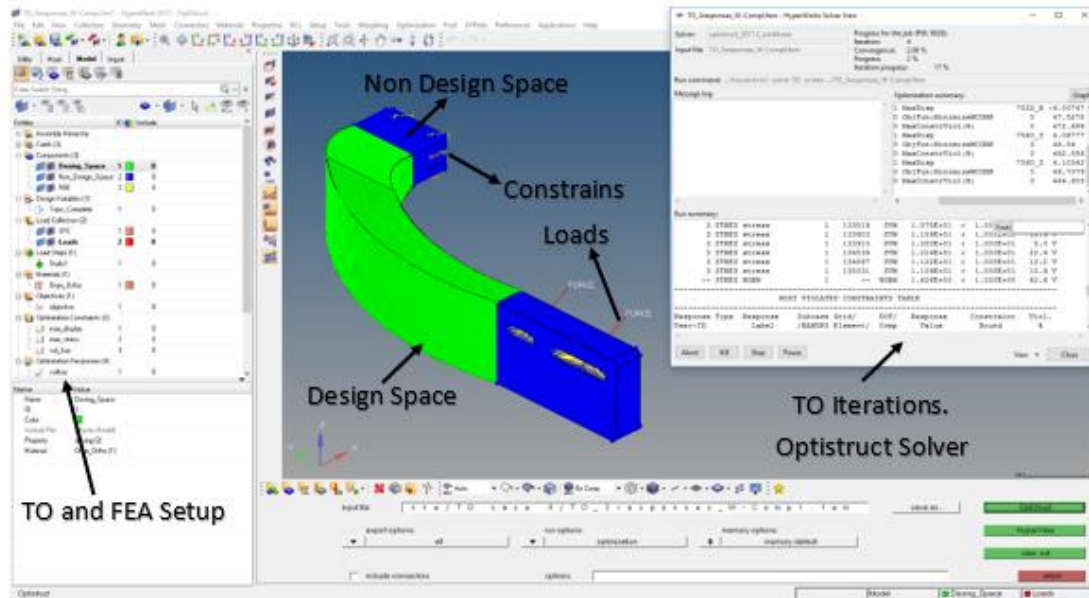


Figure 40. Hypermesh interface with TO and FEA setup for Analysis 2.

II. The design spaces were evaluated with FEM in a Topology Optimization analysis.

The TO objective was minimize the weight compliance while keeping a volume fraction less than 0.5; von misses stress less than 10 MPa, and static displacement less than 0.5 mm. Tetra elements with 0.125 of size were used as mesh parameters.

Figure 41 shows the results of the two design space geometries tested. Analysis 1 converges after 17 iterations. The FEA results show some issues in the interface between the design and non-design space, with stresses higher than 10 MPa. A new design space was proposed in Analysis 2. Analysis 2 converges after 23 iterations. The FEA results show stresses less than 10 MPa all over the part. The TO results shows structural patterns in the design. A 50% reduction in volume fraction was accomplished in the two cases.

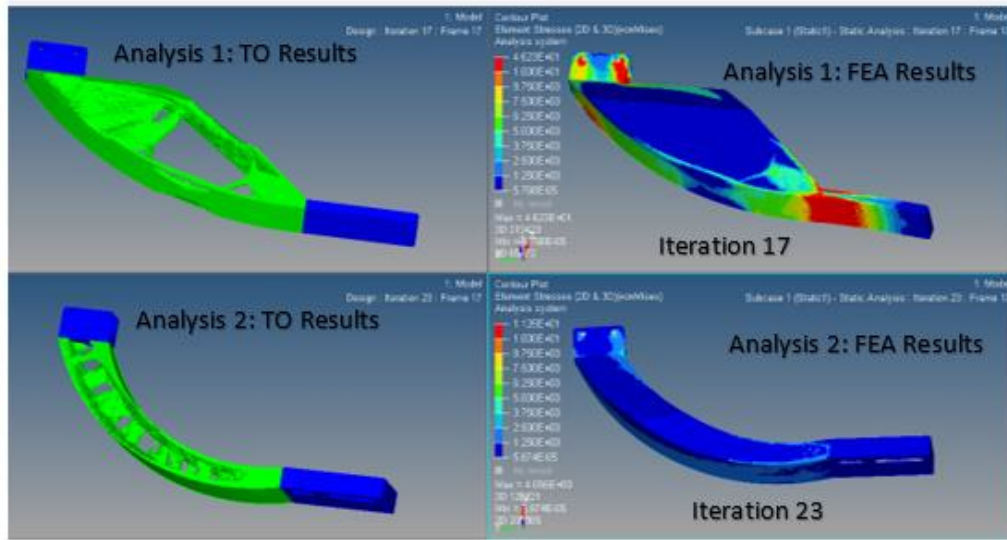


Figure 41. Overall TO and FEA results for different Design Space Geometry

III. To design the final part, Brooks and Molony recommendations were following.

From Hyperview, the TO geometries obtained were exported. However, several features and defects appear in the exported STL file. For this reason, the bracket was designed in NX 10, following the TO findings obtained in the two analyses. Figure 42a shows the CAD proposed for the bracket. Figure 42b shows the reinforced zones. The carbon fiber strands were fixed according to Brooks and Molony methodology.

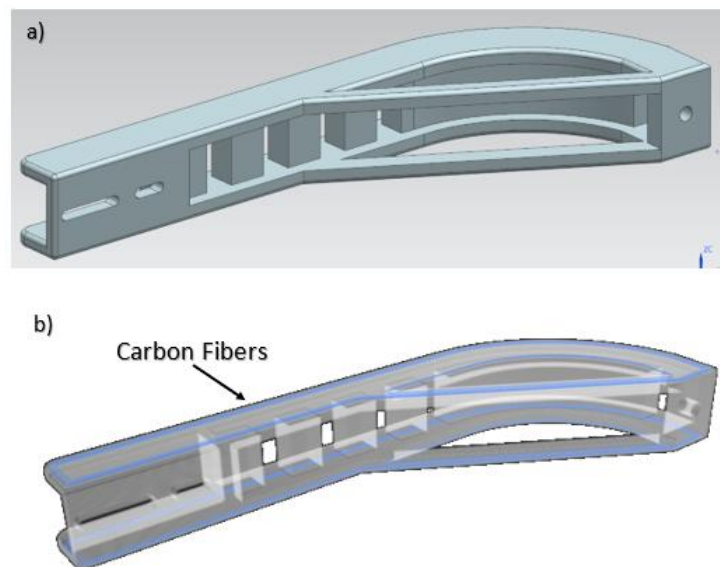


Figure 42. Optimized Bracket for Vision System. a) CAD b) Slicing software Setup

IV. Finally, the optimized bracket was manufacturing using the design guidelines proposed in this thesis work.

For the final assembly, two symmetrical brackets were printed. A central base, that connects the two brackets was also designed and printed. Figure 43 shows the 3D printed bracket and the final assembly of the Vision system. The next settings were used during the manufacturing process:

- Onyx was used as matrix material, while continuous carbon fibers were used to reinforce the components.
- For all the parts, a Triangular infill pattern and a 25% of infill density were used.
- To reinforce the bracket (232 layers), just 8 layers were added with carbon fiber rings. Three concentric rings were added in each layer preferring a wider arrangement.
- The start point of reinforcement was moving by 10% over the 8 layers reinforced, fixing the points in a distributed manner.

The printing time for one bracket was 11.5 h, and the material cost was \$27.50 dollars. The overall system was printed in 37 h, and the material cost for all the parts was \$76.61 dollars.

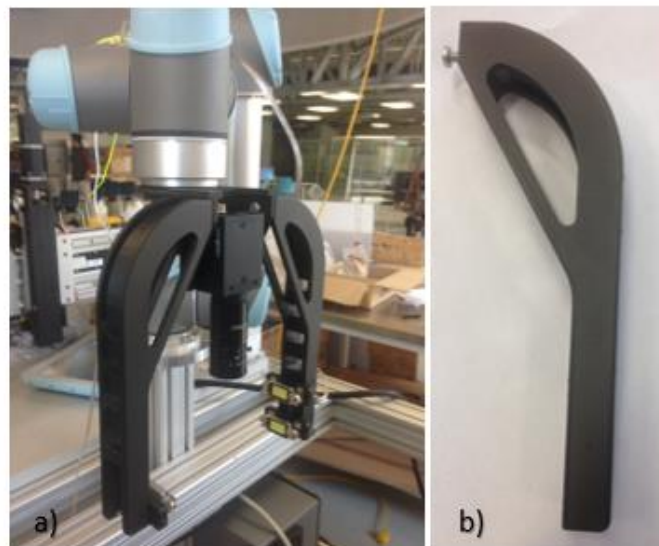


Figure 43. Smart Vision System a) Final Assembly b) Printed bracket

Chapter 7: Conclusions and Future Work

7.1 Conclusions

In this work, 3D printed composites with continuous carbon fiber reinforcement and chopped (Onyx) composites were built and tested. Some design guidelines for infill density and infill pattern were found. The influence of fiber volume fraction (VF) and fiber placement arrangement on continuous carbon fiber (CF) reinforcement composites were studied. Also, the effect of the initial point of the reinforcement fiber in the tensile properties was evaluated.

Onyx samples show small improvements with respect to Nylon. The Triangular shape has a better tensile performance due to the higher contact between stacked strands and, more importantly, due to the alignment of strands in the tensile direction. As a consequence, this arrangement should be used whenever possible.

The influence of fiber volume fraction (VF) and fiber printing architecture on continuous carbon fiber reinforcement composites were measured. From the comparison of the two printing architecture (1R vs. 3R) in the same volume fraction, it was shown the arrangement of fibers has an effect on tensile properties with a slightly better performance for the wider arrangement. As expected, the tensile properties of CFR composites have much better performance when the amount of fiber is increased.

Two different fracture mechanisms for CFR composites were studied. The influence of the elastic modulus and the tensile strength, when the initial point of the reinforcement fiber is moved, were also reported. Fix the initial point of fiber in a distributed manner was the best option to increase the tensile properties.

A variation of the Rule of Mixtures method to predict elastic modulus for CFR composites with lower fiber content that considering different geometric characteristics was proposed. Good correspondence between theoretical and experimental data was found for volume fractions smaller than 11%.

7.2 Future Work

To increase the reliability of the 3D printed composite, more mechanical characterization is needed. To a better understanding of the final mechanical performance others mechanical tests must be performed. Perform torsion and compression test is recommended. Even fatigue test must be completed for end use engineering parts.

Today, Topology Optimization (TO) for Additive Manufacturing is a very important topic for research. Some exploratory experiments were conducted to analyze an “Adding” TO approach. For future work, the creation of a TO algorithm, that includes the use of Deep learning (Neural Networks/ Genetic Algorithms) for 3D printing composite is proposed.

Proposed future work, also includes the observation of the fiber behavior evolution of 3D printed carbon fiber and fiberglass composites under uniaxial tension using Computer Tomography (CT). The goal would be to measure and observe irregularities, such as first fiber strands broken, void areas or non-uniform distribution of the thickness strands. Of particular interest is to determine the “load elastic limit,” when the first critical defects appear in this kind of composite specimens.

Other future work is to create a mathematical model that integrates the Melenka’s method with the Rule of Mixture approach presented in this work. This method must be tested for a range of lower and larger fiber reinforcement volume fraction. New materials, like Kevlar or Fiberglass, must also be considered.

Bibliography

- [1] T. Wohlers, "Wohlers Report 2015, Wohlers Associates, 2015."
- [2] Naranjo J, Ahuett H, Guemes D, Orta P, "Prospective Study for the Deployment of AM at Bocar," Monterrey, 2017.
- [3] Z. K. Awad, T. Aravinthan, Y. Zhuge, and F. Gonzalez, "A review of optimization techniques used in the design of fibre composite structures for civil engineering applications," *Mater. Des.*, vol. 33, no. 1, pp. 534–544, 2012.
- [4] B. Saenz, P. Zepeda, I. Guadalupe, and G. Salazar, "Manufactura aditiva en metales," 2016.
- [5] Mallick P., *Fiber- Reinforced Composites*, Third. CRC Press, 2007.
- [6] A. Armillotta, R. Baraggi, and S. Fasoli, "SLM tooling for die casting with conformal cooling channels," *Int. J. Adv. Manuf. Technol.*, vol. 71, no. 1–4, pp. 573–583, 2014.
- [7] E. W. Hovig, V. Brøtan, and K. Sørby, "Additive Manufacturing for Enhanced Cooling in Moulds for Casting," no. Iwama, pp. 59–62, 2016.
- [8] R. Hölker and A. E. Tekkaya, "Advancements in the manufacturing of dies for hot aluminum extrusion with conformal cooling channels," *Int. J. Adv. Manuf. Technol.*, vol. 83, no. 5–8, pp. 1209–1220, 2016.
- [9] R. Hölker, A. Jäger, N. Ben Khalifa, and A. E. Tekkaya, "Controlling heat balance in hot aluminum extrusion by additive manufactured extrusion dies with conformal cooling channels," *Int. J. Precis. Eng. Manuf.*, vol. 14, no. 8, pp. 1487–1493, 2013.
- [10] E. Atzeni and A. Salmi, "Economics of additive manufacturing for end-usable metal parts," *Int. J. Adv. Manuf. Technol.*, vol. 62, no. 9–12, pp. 1147–1155, 2012.
- [11] M. K. Thompson, G. Moroni, T. Vaneker, G. Fadel, R. I. Campbell, I. Gibson, A. Bernard, J. Schulz, P. Graf, B. Ahuja, and F. Martina, "Design for Additive Manufacturing: Trends, opportunities, considerations, and constraints," *CIRP Ann. - Manuf. Technol.*, vol. 65, no. 2, pp. 737–760, 2016.
- [12] D. Zhang, Q. Cai, J. Liu, and R. Li, "Research on process and microstructure formation of W-Ni-Fe alloy fabricated by Selective Laser melting," *J. Mater. Eng. Perform.*, vol. 20, no. 6, pp. 1049–1054, 2011.
- [13] B. Nie, L. Yang, H. Huang, S. Bai, P. Wan, and J. Liu, "Femtosecond laser additive manufacturing of iron and tungsten parts," *Appl. Phys. A Mater. Sci. Process.*, vol. 119, no. 3, pp. 1075–1080, 2015.
- [14] R. Li, Y. Shi, J. Liu, Z. Xie, and Z. Wang, "Selective laser melting W-10 wt.% Cu composite powders," *Int. J. Adv. Manuf. Technol.*, vol. 48, no. 5–8, pp. 597–605, 2010.
- [15] Dr. Jason Jones and Peter Coates, "7 Families of Additive Manufacturing (ASTM F2792)," 2015.
- [16] K. V. Wong and A. Hernandez, "A Review of Additive Manufacturing," *ISRN Mech. Eng.*, vol. 2012, pp. 1–10, 2012.

- [17] A. M. Siliceo A, Villarreal A, Parra R, Lara M, Cazares D, "CASOS DE ESTUDIO: Inserto, Jigs & Fixtures en PROSPECTIVA TECNOLÓGICA DE AM," 2017.
- [18] L. M. Mendoza E, Pascual L, Robles J, Aragon F, Martinez G, "CASOS DE ESTUDIO: Producto & Prototipo en PROSPECTIVA TECNOLÓGICA DE AM," 2017.
- [19] F. ILT, "Tools Made out of Combined Materials," 2014.
- [20] L. E. Murr, S. M. Gaytan, A. Ceylan, E. Martinez, J. L. Martinez, D. H. Hernandez, B. I. Machado, D. A. Ramirez, F. Medina, S. Collins, and R. B. Wicker, "Characterization of titanium aluminide alloy components fabricated by additive manufacturing using electron beam melting," *Acta Mater.*, vol. 58, no. 5, pp. 1887–1894, 2010.
- [21] W. E. Frazier, "Metal additive manufacturing: A review," *J. Mater. Eng. Perform.*, vol. 23, no. 6, pp. 1917–1928, 2014.
- [22] Stratasys, "3D PRINTING WITH CARBON FIBER," 2018. [Online]. Available: <http://www.stratasys.com/es-mx/nylon12cf>.
- [23] H. Prüß and T. Vietor, "Design for Fiber-Reinforced Additive Manufacturing," *J. Mech. Des.*, vol. 137, no. 11, p. 111409, 2015.
- [24] F. Baumann, J. Scholz, and J. Fleischer, "Investigation of a New Approach for Additively Manufactured Continuous Fiber-reinforced Polymers," *Procedia CIRP*, vol. 66, pp. 323–328, 2017.
- [25] G. T. Mark, "Apparatus for Fiber Reinforced Additive Manufacturing Pub. No.: US 2013/0284069 A1," 2013.
- [26] G. T. Mark, "Methods for Fiber Reinforced Additive Manufacturing Application Publication," vol. 1, no. 19, 2014.
- [27] A. N. Dickson, J. N. Barry, K. A. McDonnell, and D. P. Dowling, "Fabrication of continuous carbon, glass and Kevlar fibre reinforced polymer composites using additive manufacturing," *Addit. Manuf.*, vol. 16, pp. 146–152, 2017.
- [28] G. W. Melenka, B. K. O. Cheung, J. S. Schofield, M. R. Dawson, and J. P. Carey, "Evaluation and prediction of the tensile properties of continuous fiber-reinforced 3D printed structures," *Compos. Struct.*, vol. 153, pp. 866–875, 2016.
- [29] F. Van Der Klift, Y. Koga, A. Todoroki, M. Ueda, Y. Hirano, and R. Matsuzaki, "3D Printing of Continuous Carbon Fibre Reinforced Thermo-Plastic (CFRTP) Tensile Test Specimens," *Open J. Compos. Mater.*, vol. 6, no. 1, pp. 18–27, 2016.
- [30] S. Christ, M. Schnabel, E. Vorndran, J. J. Groll, and U. Gbureck, "Fiber reinforcement during 3D printing," *Mater. Lett.*, vol. 139, pp. 165–168, 2015.
- [31] C. Yang, X. Tian, T. Liu, Y. Cao, and D. Li, "3D printing for continuous fiber reinforced thermoplastic composites: mechanism and performance," *Rapid Prototyp. J.*, vol. 23, no. 1, pp. 209–215, 2017.
- [32] C. C. Spackman, C. R. Frank, K. C. Picha, and J. Samuel, "3D printing of fiber-reinforced soft composites: Process study and material characterization," *J. Manuf.*

- Process.*, vol. 23, pp. 296–305, 2016.
- [33] F. Ning, W. Cong, Y. Hu, and H. Wang, “Additive manufacturing of carbon fiber-reinforced plastic composites using fused deposition modeling: Effects of process parameters on tensile properties,” *J. Compos. Mater.*, 2016.
 - [34] D. A. Arcos-Novillo and D. Güemes-Castorena, “Development of an Additive Manufacturing Technology Scenario for Opportunity Identification—The case of Mexico,” *Futures*, vol. 90, no. May, pp. 1–15, 2017.
 - [35] C. Klahn, B. Leutenecker, and M. Meboldt, “Design Strategies for the Process of Additive Manufacturing,” vol. 36, pp. 230–235, 2015.
 - [36] W. Tao, “2016 International Symposium on Flexible Automation,” pp. 1–3, 2016.
 - [37] H. Brooks and S. Molony, “Design and evaluation of additively manufactured parts with three dimensional continuous fibre reinforcement,” vol. 90, pp. 276–283, 2016.
 - [38] Markforged, “MATERIAL SPECIFICATIONS COMPOSITES,” 2018. [Online]. Available: https://static.markforged.com/markforged_composites_datasheet.pdf. [Accessed: 12-Feb-2018].
 - [39] ASTM International, “Standard test method for tensile properties of plastics,” *ASTM Int.*, vol. 8, pp. 46–58, 2003.
 - [40] F. Report, “Tabbing Guide for Composite Test Specimens,” no. October, 2002.
 - [41] Thermo Scientific, “Introduction to FT-IR Sample Handling,” *Thermo Fischer Sci. Inc.*, 2013.
 - [42] M. K. Agarwala, V. R. Jamalabad, N. A. Langrana, A. Safari, P. J. Whalen, and S. C. Danforth, “Structural quality of parts processed by fused deposition,” *Rapid Prototyp. J.*, vol. 2, no. 4, pp. 4–19, 1996.
 - [43] J. F. Rodríguez, J. P. Thomas, and J. E. Renaud, “Characterization of the mesostructure of fused-deposition acrylonitrile-butadiene-styrene materials,” *Rapid Prototyp. J.*, vol. 6, no. 3, pp. 175–186, 2000.
 - [44] J. F. Rodríguez, J. P. Thomas, and J. E. Renaud, “Mechanical behavior of acrylonitrile butadiene styrene fused deposition materials modeling,” *Rapid Prototyp. J.*, vol. 9, no. 4, pp. 219–230, 2003.
 - [45] Q. Sun, G. M. Rizvi, C. T. Bellehumeur, and P. Gu, “Effect of processing conditions on the bonding quality of FDM polymer filaments,” *Rapid Prototyp. J.*, vol. 14, no. 2, pp. 72–80, 2008.
 - [46] A. M. D. S. Matweb, “Aluminium 6061-T6,” *Matweb*, 2000. [Online]. Available: <http://asm.matweb.com/search/SpecificMaterial.asp?bassnum=ma6061t6>. [Accessed: 15-Nov-2017].
 - [47] B. H. Stuart, *Infrared Spectroscopy: Fundamentals and Applications*, vol. 8. 2004.
 - [48] Institute of Chemical Physics, “Polyamide (Nylon 6) – Database of ATR-FT-IR spectra of various materials,” 2018. [Online]. Available: http://lisa.chem.ut.ee/IR_spectra/textile-fibres/polyamide/. [Accessed: 16-Mar-2018].

- [49] C. Freitag, R. Weber, and T. Graf, "Polarization dependence of laser interaction with carbon fibers and CFRP," *Opt. Express*, vol. 22, no. 2, p. 1474, 2014.
- [50] H. Xu, J. Hu, and Z. Yu, "Absorption behavior analysis of Carbon Fiber Reinforced Polymer in laser processing," *Opt. Mater. Express*, vol. 5, no. 10, p. 2330, 2015.
- [51] Dutch Filaments, "CARBON-P Datasheet," 2015.
- [52] Markforged, "Mechanical properties of continuous fibers," 2016. [Online]. Available: https://bastech.com/wp-content/uploads/2016/05/MF_Mark-Two-3D-Printer-DS-Web.pdf. [Accessed: 15-Nov-2017].
- [53] W. W. Bunse B, Kagermann H, "Industry 4.0: Smart manufacturing for the future," *Ger. Trade Invest*, 2014.
- [54] H. Ahuett-Garza and T. Kurfess, "A brief discussion on the trends of habilitating technologies for Industry 4.0 and Smart Manufacturing," *Manuf. Lett.*, pp. 2–5, 2018.
- [55] J. E. Shigley, C. R. Mischke, and R. G. Budynas, *Mechanical Engineering Design*, vol. New York,. 2002.
- [56] U. Galan, P. Orta, T. Kurfess, and H. Ahuett-Garza, "Surface defect identification and measurement for metal castings by vision system," *Manuf. Lett.*, vol. 15, pp. 5–8, 2018.
- [57] A. Bellini and S. Güçer, "Mechanical Characterization of parts fabricated using fused deposition modeling," *Rapid Prototyp.*, vol. 9, no. 4, pp. 252–264, 2003.

Appendix A: Abbreviations and acronyms

Table A.1 Abbreviations

	Description
AM	A dditive M anufacturing
CFR	C ontinuous F iber R einforcement
ANOVA	A nalysis of V ariance
FEA	F inite E lement A nalysis
TO	T opology O ptimization
DMLS	D irect m etal l aser s intering
EBM	E lectron B eam M elting
FDM	F used d eposition m odeling
LENS	L aser e ngineered n et s haping
SL	S tereolithography
SLM	S elective laser m elting
SLS	S elective laser s intering
STL	file format native to the Stereolithography CAD software

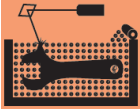



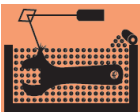

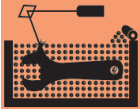

Appendix B: Variables and Symbols

Table B.1 Variables and Symbols





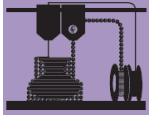
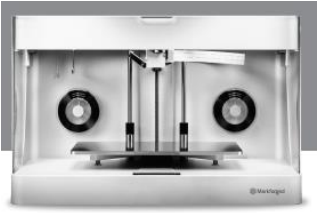
E_{matrix}	Matrix elastic modulus
E_{fiber}	Fiber elastic modulus
Φ_{fiber}	Fiber volume fraction
Φ_{matrix}	Matrix volume fraction
V_i	Region volumes
$V_{composite}$	Overall volume
$E_{predicted}$	Predicted elastic modulus
W_{wall}	Wall strand width
W	Overall width
W_{fiber}	Fiber strand width
T	Overall thickness
T_{layer}	Layer thickness
H	Tensile length
N	Total number of layers
N_{walls}	Number of wall rings
N_{floor}	Number of floor layers
N_{roof}	Number of roof layers
N_{fiber}	Number of reinforced layers
R_{fiber}	Number of Reinforced rings

ANNEX 1: AM Manufactures and Equipment



Supplier	Application	AM Technology	Machine	Specific Application	Pictures	Contact
EOS	Polymer/ Plastics		FORMIGA P 110	Production/ Prototyping		Neil Lehman/Sam Houston neil.lehman@eos-na.com sam.houston@eos-na.com Global: +1 254 743-3080 3115 Lucius McCelvey Temple, Tx, 76504 USA US.materialorders@eos-na.com
			EOS P 396	Production		
			EOSINT P 800	Production/ Prototyping		
			EOS P 770	Production		
	Metal		EOS M 100	Production		
			EOS M 290	Production		
			EOS M 400	Production		
			EOS M 400-4	Production		
			EOSINT M 280	Prototyping/ Tool Inserts		
			PRECIOUS M 080	Jewelry		
3D SYSTEMS	Polymer/ Plastics		ProJet® 6000 HD	Production/Prototyping		Americas Toll Free (U.S./Canada): +1 888.598.1438 Global: +1 803.326.3930 support-us@3dsystems.com
			ProJet® 7000 HD	Prototypes/ End-use parts		
			ProX® 800	Prototypes/ Rapid tooling		
			ProX® 950	Production/End-use parts		
			ProX® SLS 500	Prototypes/End-use parts		
			sPro™ 140	Production		
			sPro™ 230	Production		
			sPro™ 60 HD	Production		

3D SYSTEMS	Metal	Direct Metal Printing (DMP) 	ProX® DMP 100	Production/tooling /tooling insert		
			ProX® DMP 100 Dental	Production/ dental prostheses		
			ProX® DMP 200	Production		
			ProX® DMP 200 Dental	Production/ dental prostheses		
			ProX® DMP 300	Production		
			ProX® DMP 320	Production		
EXONE	Metal	Binder Jetting 	Exerial	Production		The ExOne Company 127 Industry Boulevard North Huntingdon, PA 15642 USA T +1 724 765 1349 M +1 724 552 8345 www.exone.com
			S-Max	Production/ Prototyping		
			S-Print	Production/ Prototyping		
			M-Print	Production		
			M-Flex	Production/ Prototyping		
			Innovent	Research & Education Printers		
			M-Flex	Research & Education Printers		
Renishaw	Metal	Laser Sintering SLS 	RenAM 500M	Production		Stone Business Park, Brooms Road, Stone Staffordshire, ST15 0SH United Kingdom T +44 (0) 1785 285000 F +44 (0) 1785 285001 www.renishaw.com
			AM 400	Production		
			AM 250	Production		
SLM Solutions	Metal	Selective Laser Melting SLM 	SLM®500HL	Production/ Prototyping		SLM Solutions Group AG Roggenhorster Strasse 9c 23556 Lübeck Germany Telephone: +49-451- 16082-0 Fax: +49-451- 16082-250
			SLM®280HL	Production/ Prototyping		
			SLM®125HL	Production		

ARCAM	Metal	<div>Electron Beam Melting EBM</div> 	Arcam Q10plus	Orthopedic implants		Arcam AB, Headquarters Krokslätts Fabriker 27A SE-431 37 Mölndal Sweden Phone: +46 (0)31 710 32 00
			Arcam Q20plus	Aerospace Components		
			Arcam A2X	Aerospace Components		
Realizer	Metal	<div>Selective Laser Melting SLM</div> 	SLM 50	Jewellery		Hauptstrasse 35 33178 Borcheln, Germany Phone: (0 52 51) 69 87 9 - 0 Fax: (0 52 51) 69 87 9 - 99
			SLM 125	Production		
			SLM300I	Research & Education Printers		
Stratasys	Polymer/ Plastics	<div>Fused deposition modeling FDM</div> 	Fortus 380mc	Production parts, manufacturing tools, rapid prototyping		Mexico Jaime Balmes 11 Int 301 Torre D Polanco, Miguel Hidalgo 11510 Estado de México. Phone: +52-5580-4184
			Fortus 450mc	Production parts, manufacturing tools, rapid prototyping		
			Fortus 900mc	Production parts, manufacturing tools, rapid prototyping		
		<div>Polyjet</div> 	Objet1000 Plus	Production		
			Stratasys J750	Production		

CONCEPT Laser	Metal	LaserCUSING - Laser melting 	Mlab cusing	Research & Education Printers		Concept Laser GmbH An der Zeil 8 96215 Lichtenfels Germany P +49 (0) 9571 1679-0 F +49 (0) 9571 1679-499
			M1 cusing	Production/Prototyping		
			M2 cusing	Production		
			X line 2000R	Production		
Optomec	Metal	Laser Engineered Net Shaping (LENS) systems 	LENS 450	Repair applications for small parts.		Optomec 3911 Singer N.E. Albuquerque, NM 87109 Phone: (505) 761-8250 Web: http://www.optomec.com
			LENS MR-7	Production		
			LENS 850-R	Production		
Markforged	Polymer/ Plastics	Fused Filament Fabrication (FFF) 	Mark Two	Research/ Prototyping		Ing. Miguel Mondragón Muñoz Tecnologías y Soluciones Tridimensionales SA de CV Tel. (81) 8332 2125 mmondragon@tecsol3d.co
			MarkX	Production/ Prototyping		
			Onyx / Onyx Pro	Production/ Prototyping		

	Metal	<p>ADAM Atomic Diffusion Additive Manufacturing</p> 	Metal X	Production/ Prototyping		
TRUMPF	Metal	<p>LMF Laser Metal Fusion</p> 	Truprint 1000	Prototyping		<p>TRUMPF Inc. Farmington Industrial Park Farmington, CT 06032 USA Tel.: +1 (860) 255-6000</p>
			Truprint 3000	Production		
			TruLaser Cell 300	Production/ Prototyping		
CARBON 3D	Polymer/ Plastics	<p>DLS (Digital Light Synthesis)</p> 	Carbon SpeedCell™ M1 Printer	Prototyping		<p>1089 Mills Way, Redwood City, CA 94063 USA Tel.: +1 (650) 285-6307 info@carbon3d.com pr@carbon3d.com</p>
			Carbon SpeedCell™ M2 Printer	Production/ Prototyping		

DESKTOP METAL	Metal	Bound Metal Deposition (BMD)	Studio System	Production/ Prototyping		63 Third Avenue, Burlington, MA 01803 USA Tel.: +1 978-224-1244 sales@desktopmetal.com
			Production System	Production		

ANNEX 2: Hybrid Technologies

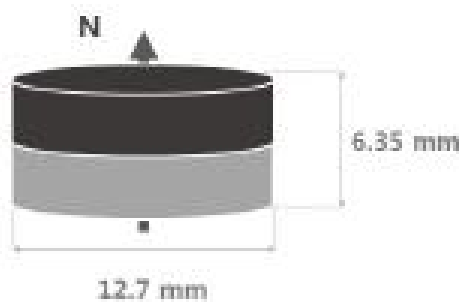
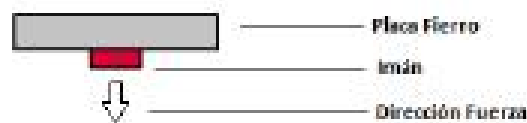
<i>Supplier</i>	<i>System</i>	<i>AM Technology</i>	<i>Work Volume</i>	<i>Materials</i>	<i>Resolution</i>	<i>Observations</i>
Hybrid Manufacturing Technologies	AMBIT™	Tool Changeable Laser Cladding	Depend on CNC machine	Depend on CNC machine	Depend on CNC machine	A series of deposition heads and docking systems which allows virtually any CNC machine (or robotic platform) to use non-traditional processing heads in the spindle and conveniently change between them.
OPTOMECH	LENS 3D METAL HYBRID	Metal deposition by powder nozzle	Machining = 20"x14"x20" (500x350x500 mm) Deposition = 14x14x20" (350x350x500 mm)	Tool and Stainless Steels, Inconels, Hastelloy, Stellite, Tungsten Carbide	0.0001" (2.5 microns)	The system utilizes Optomech industry proven LENS Print Engine technology seamlessly integrated into Class 1 Laser Safe CNC platform
DMG MORI	LASERTEC 65	Laser Deposition Welding & Milling	up to ø 23.6 in., 15.7 in. height	Stainless Steel Nickel-Based Alloys Tungsten Carbide Matrix Materials Bronze and Brass Alloys Chrome-Cobalt-Molybdenum Stellite Tool Steel	Wall thickness from 0.004 to 0.2 in.	This innovative hybrid-solution combines the flexibility of the laser metal deposition process with the precision of the cutting process and in addition to that allows additive manufacturing in milling quality.
MITSUBISHI CORP.	LUMEX AVANCE 25	Fusing metal laser sintering (3D SLS)	9.8 x 9.8 in (250 x 250) mm	HR Steel Maraging Steel (52Rc after Heat Treat) 630 Stainless Steel 316L Stainless Steel	S/I	The LUMEX Avance-25, one-process manufacturing of complex molds and parts by fusing metal laser sintering (3D SLS) technology with high-speed milling technology.
MAZAK	INTEGREX i-400AM	Lase Cladding	Not specified	Inconel® 718 and 316 stainless steel.	Milling spindles provide -30/+120-degree B-axis movement	As a fusion of additive technology and the most advanced Multi-Tasking capabilities, the INTEGREX i-400AM (additive manufacturing) represents a highly innovative alternative to conventional processing regarding part design and machining.

ANNEX 3: Datasheet Magnets (ND143)

IMAN DE NEODIMIO ND143

ID DEL ARTICULO	ND143
MATERIAL	NdFeB
DIÁMETRO	1/2" (12.7 mm)
ESPESOR	1/4" (6.35 mm)
TOLERANCIA DIMENSIONES	+/- 0.1 mm
GRADO	N35
FUERZA DE SUJECIÓN	3.9 Kg APROX *
TIPO DE MAGNETIZACIÓN	AXIAL
RECUBRIMIENTO	Ni-Cu-Ni NÍQUEL
MAX TEMP. DE OPERACIÓN	80° C
DISPONIBILIDAD	ENTREGA INMEDIATA

* Detalle de calculo para la fuerza de sujeción.



PREGUNTAS | COTIZACIONES

Curriculum Vitae

Juan Miguel Naranjo Lozada was born in Ambato, Ecuador, on April 21, 1989. He earned the Mechatronic Engineering degree from the *Instituto Tecnológico y de Estudios Superiores de Monterrey*, Toluca Campus in December 2011. He was accepted in the graduate programs in Manufacturing System at *Instituto Tecnológico y de Estudios Superiores de Monterrey*, Monterrey Campus in August 2016.

This document was typed in using Microsoft Word by Juan Miguel Naranjo Lozada